Biogeosciences, 18, 1269–1289, 2021
https://doi.org/10.5194/bg-18-1269-2021

Biogeosciences
Open Access

Reviews and syntheses: The biogeochemical cycle of silicon in the modern ocean

Paul J. Tréguer[1,2], Jill N. Sutton[1], Mark Brzezinski[3], Matthew A. Charette[4], Timothy Devries[5], Stephanie Dutkiewicz[6], Claudia Ehlert[7], Jon Hawkings[8,9], Aude Leynaert[1], Su Mei Liu[10,11], Natalia Llopis Monferrer[1], María López-Acosta[12,13], Manuel Maldonado[13], Shaily Rahman[14], Lihua Ran[15], and Olivier Rouxel[16]

[1]Univ Brest, CNRS, IRD, Ifremer, Institut Universitaire Européen de la Mer, LEMAR, Rue Dumont d'Urville, 29280, Plouzané, France
[2]State Key Laboratory of Satellite Ocean Dynamics (SOED), Ministry of Natural Resource, Hangzhou 310012, China
[3]Marine Science Institute, University of California, Santa Barbara, CA, USA
[4]Department of Marine Chemistry and Geochemistry, Woods Hole Oceanographic Institution, Woods Hole, MA 02543, USA
[5]Department of Geography, University of California, Santa Barbara, CA, USA
[6]Department of Earth, Atmospheric and Planetary Sciences (DEAPS), Massachusetts Institute of Technology (MIT), Cambridge, MA 02139, USA
[7]Research Group for Marine Isotope Geochemistry, Institute for Chemistry and Biology of the Marine Environment (ICBM), Carl von Ossietzky University of Oldenburg, Oldenburg, Germany
[8]National High Magnetic Field Lab and Earth, Ocean and Atmospheric Sciences, Florida State University, Tallahassee, USA
[9]Interface Geochemistry, German Research Centre for Geosciences GFZ, Potsdam, Germany
[10]Frontiers Science Center for Deep Ocean Multispheres and Earth System, and Laboratory of Marine Chemistry Theory and Technology MOEy, Ocean University of China, Qingdao 266100, China
[11]Laboratory for Marine Ecology and Environmental Science, Qingdao National Laboratory for Marine Science and Technology, Qingdao 266237, China
[12]Institute of Marine Research (IIM-CSIC), Rúa de Eduardo Cabello 6, Vigo 36208, Pontevedra, Spain
[13]Department of Marine Ecology. Center for Advanced Studies of Blanes (CEAB-CSIC), Acceso Cala St. Francesc 14, Blanes 17300, Girona, Spain
[14]School of Ocean Science and Engineering, University of Southern Mississippi, Stennis Space Center, MS 39529, USA
[15]Key Laboratory of Marine Ecosystem Dynamics, Second Institute of Oceanography, Ministry of Natural Resources, P. R. China
[16]IFREMER, Centre de Brest, Technopôle Brest Iroise, Plouzané, France

Correspondence: Paul Tréguer (paul.treguer@univ-brest.fr) and Jill Sutton (jill.sutton@univ-brest.fr)

Received: 20 July 2020 – Discussion started: 3 August 2020
Revised: 18 December 2020 – Accepted: 23 December 2020 – Published: 18 February 2021

Abstract. The element silicon (Si) is required for the growth of silicified organisms in marine environments, such as diatoms. These organisms consume vast amounts of Si together with N, P, and C, connecting the biogeochemical cycles of these elements. Thus, understanding the Si cycle in the ocean is critical for understanding wider issues such as carbon sequestration by the ocean's biological pump. In this review, we show that recent advances in process studies indicate that total Si inputs and outputs, to and from the world ocean, are 57 % and 37 % higher, respectively, than previous estimates. We also update the total ocean silicic acid inventory value, which is about 24 % higher than previously estimated. These changes are significant, modifying factors such as the geochemical residence time of Si, which is now about 8000 years, 2 times faster than previously assumed. In addition, we present an updated value of the global annual pelagic biogenic silica production (255 Tmol Si yr^{-1}) based on new data from 49 field studies and 18 model outputs, and we provide a first estimate of the global annual benthic biogenic silica production due to sponges (6 Tmol Si yr^{-1}). Given these important modifications, we hypothesize that the modern ocean Si cycle is at approximately steady state with inputs = 14.8(±2.6) Tmol Si yr^{-1} and outputs = 15.6(±2.4) Tmol Si yr^{-1}. Potential impacts of global change on the marine Si cycle are discussed.

1 Introduction

Silicon, the seventh most abundant element in the universe, is the second most abundant element in the Earth's crust. The weathering of the Earth's crust by CO_2-rich rainwater, a key process in the control of atmospheric CO_2 (Berner et al., 1983; Wollast and Mackenzie, 1989), results in the generation of silicic acid (dSi; $Si(OH)_4$) in aqueous environments. Silicifiers are among the most important aquatic organisms and include micro-organisms (e.g., diatoms, rhizarians, silicoflagellates, several species of choanoflagellates) and macro-organisms (e.g., siliceous sponges). Silicifiers use dSi to precipitate biogenic silica (bSi; SiO_2) as internal (Moriceau et al., 2019) and/or external (Maldonado et al., 2019) structures. Phototrophic silicifiers, such as diatoms, globally consume vast amounts of Si concomitantly with nitrogen (N), phosphorus (P), and inorganic carbon (C), connecting the biogeochemistry of these elements and contributing to the sequestration of atmospheric CO_2 in the ocean (Tréguer and Pondaven, 2000). Heterotrophic organisms like rhizarians, choanoflagellates, and sponges produce bSi independently of the photoautotrophic processing of C and N (Maldonado et al., 2012, 2019; Llopis Monferrer et al., 2020).

Understanding the Si cycle is critical for understanding the functioning of marine food webs, biogeochemical cycles, and the biological carbon pump. Herein, we review recent advances in field observations and modeling that have changed our understanding of the global Si cycle and provide an update of four of the six net annual input fluxes and of all the output fluxes previously estimated by Tréguer and De La Rocha (2013). Taking into account numerous field studies in different marine provinces and model outputs, we re-estimate the Si production (Nelson et al., 1995), review the potential contribution of rhizarians (Llopis Monferrer et al., 2020) and picocyanobacteria (Ohnemus et al., 2016), and give an estimate of the total bSi production by siliceous sponges using recently published data on sponge bSi in marine sediments (Maldonado et al., 2019). We discuss the question of the balance and imbalance of the marine Si biogeochemical cycle at different timescales, and we hypothesize that the modern ocean Si cycle is potentially at steady state with inputs = 14.8(±2.6) Tmol Si yr^{-1} approximately balancing outputs = 15.6(±2.4) Tmol Si yr^{-1} (Fig. 1). Finally, we address the question of the potential impact of anthropogenic activities on the global Si cycle and suggest guidelines for future research endeavors.

2 Advances in input fluxes

Silicic acid is delivered to the ocean through six pathways as illustrated in Fig. 1, which all ultimately derive from the weathering of the Earth's crust (Tréguer and De La Rocha, 2013). All fluxes are given with an error of 1 standard deviation.

2.1 Riverine (F_R) and aeolian (F_A) contributions

The best estimate for the riverine input (F_R) of dSi, based on data representing 60 % of the world river discharge and a discharge-weighted average dSi riverine concentration of 158 µM − Si (Dürr et al., 2011), remains at F_{RdSi} = 6.2(±1.8) Tmol Si yr^{-1} (Tréguer and De La Rocha, 2013). However, not only dSi is transferred from the terrestrial to the riverine system, with particulate Si mobilized in crystallized or amorphous forms (Dürr et al., 2011). According to Saccone et al. (2007), the term "amorphous silica" (aSi) includes biogenic silica (bSi, from phytoliths, freshwater diatoms, sponge spicules), altered bSi, and pedogenic silicates, the three of which can have similar high solubilities and reactivities. Delivery of aSi to the fluvial system has been reviewed by Frings et al. (2016), and they suggested a value of F_{RaSi} = 1.9(±1.0) Tmol Si yr^{-1}. Therefore, total F_R = 8.1(±2.0) Tmol Si yr^{-1}.

No progress has been made regarding aeolian dust deposition into the ocean (Tegen and Kohfeld, 2006) and subsequent release of dSi via dust dissolution in seawater since Tréguer and De La Rocha (2013), who summed the flux of particulate dissolvable silica and wet deposition of dSi through precipitation. Thus, our best estimate for the aeolian flux of dSi, F_A, remains 0.5(±0.5) Tmol Si yr^{-1}.

2.2 Dissolution of minerals (F_W)

As shown in Fig. 2, the low-temperature dissolution of siliceous minerals in seawater and from sediments feeds a dSi flux, F_W, through two processes: (1) the dissolution of river-derived lithogenic particles deposited along the continental margins and shelves and (2) the dissolution of basaltic glass in seawater, processes that work mostly in deep waters. About 15–20 Gt yr^{-1} of river-derived lithogenic particles are deposited along the margins and shelves (e.g., Syvitskia et al., 2003; also see Fig. 2). Dissolution experiments with river sediments or basaltic glass in seawater showed that 0.08 %–0.17 % of the Si in the solid phase was released within a few days to months (e.g., Oelkers et al., 2011; Jones et al., 2012; Pearce et al., 2013; Morin et al., 2015). However, the high solid-to-solution ratios in these experiments increased

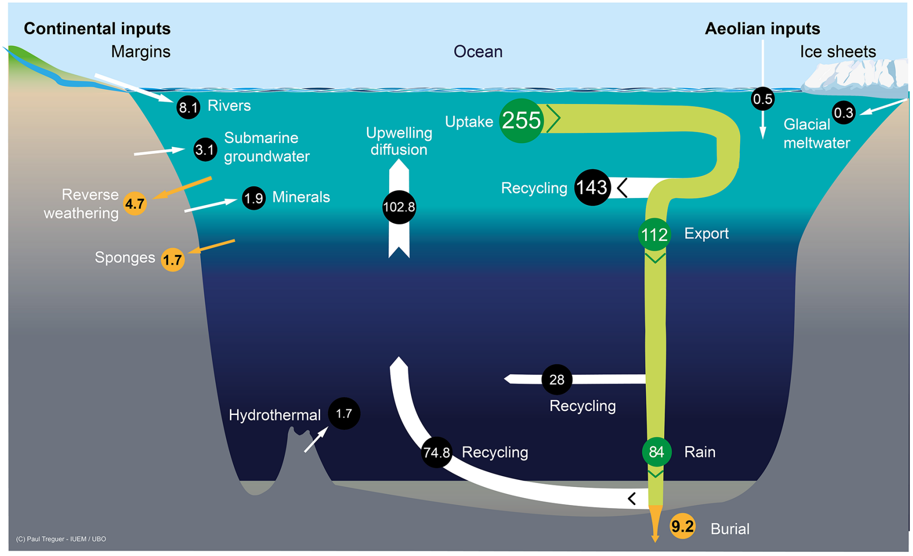

Figure 1. Schematic view of the Si cycle in the modern world ocean (input, output, and biological Si fluxes), and possible balance (total Si inputs = total Si outputs = 15.6 Tmol Si yr^{-1}) in reasonable agreement with the individual range of each flux (F); see Tables 1 and 2. The white arrows represent fluxes of net sources of silicic acid (dSi) and/or of dissolvable amorphous silica (aSi) and of dSi recycled fluxes. Orange arrows correspond to sink fluxes of Si (either as biogenic silica or as authigenic silica). Green arrows correspond to biological (pelagic) fluxes. All fluxes are in teramoles of silicon per year (Tmol Si yr^{-1}). Details are given in Sect. S1 in the Supplement.

the dSi concentration quickly to near-equilibrium conditions inhibiting further dissolution, which prevents direct comparison with natural sediments. Field observations and subsequent modeling of Si release range around 0.5 %–5 % yr^{-1} of the Si originally present in the solid phase dissolved into the seawater (e.g., Arsouze et al., 2009; Jeandel and Oelkers, 2015). On the global scale, Jeandel et al. (2011) estimated the total flux of dissolution of minerals to range between 0.7–5.4 Tmol Si yr^{-1}, i.e., similar to the dSi river flux. However, this estimate is based on the assumption of 1 %–3 % congruent dissolution of sediments for a large range of lithological composition which, so far, has not been proven.

Another approach to estimate F_W is to consider the benthic efflux from sediments devoid of biogenic silica deposits. Frings (2017) estimates that “non-biogenic-silica” sediments (i.e., clays and calcareous sediments, which cover about 78 % of the ocean area) may contribute up to 44.9 Tmol Si yr^{-1} via a benthic diffusive Si flux. However, according to lithological descriptions given in GSA Data Repository 2015271 some of the non-biogenic-silica sediment classes described in this study may contain significant bSi, which might explain this high estimate for F_W. Tréguer and De La Rocha (2013) considered benthic efflux from non-siliceous sediments ranging between ≈ 10–20 mmol m^{-2} yr^{-1} in agreement with Tréguer et al. (1995). If extrapolated to the 120 million square kilometer zone of opal-poor sediments in the global ocean, this gives an estimate of $F_W = 1.9(\pm 0.7)$ Tmol Si yr^{-1}.

2.3 Submarine groundwater (F_{GW})

Since 2013, several papers have sought to quantify the global oceanic input of dissolved Si (dSi) from submarine groundwater discharge (SGD), which includes terrestrial (freshwater) and marine (saltwater) components (Fig. 2). Silicic acid inputs through SGD may be considerable, similar to or in excess of riverine input in some places. For instance, Georg et al. (2009) estimated this input to be 0.093 Tmol Si yr^{-1} in the Bay of Bengal, which is ≈ 66 % of the Ganges–Brahmaputra river flux of dSi to the ocean. At a global scale the best estimate of Tréguer and De La Rocha (2013) for F_{GW} was 0.6(±0.6) Tmol Si yr^{-1}. More recently, Rahman et al. (2019) used a global terrestrial SGD flux model weighted according to aquifer lithology (Beck et al., 2013) in combination with a compilation of dSi in shallow water coastal aquifers to derive a terrestrial groundwater input of dSi to the world ocean of 0.7(±0.1) Tmol Si yr^{-1}. This new estimate, with its relatively low uncertainty, represents the lower limit flux of dSi to the ocean via SGD. The marine component of SGD, driven by a range of physical processes such as density gradients or waves and tides, is fed by seawater that circulates through coastal aquifers or beaches via advective flow paths (Fig. 2; also see Fig. 1 of Li et al., 1999). This circulating seawater may become enriched in dSi through bSi or mineral dissolution, the degree of enrichment being determined by subsurface residence time and mineral type (Techer et al., 2001; Anschutz et al., 2009; Ehlert et al. 2016a).

Several lines of evidence show that the mineral dissolution (strictly corresponding to net dSi input) may be sub-

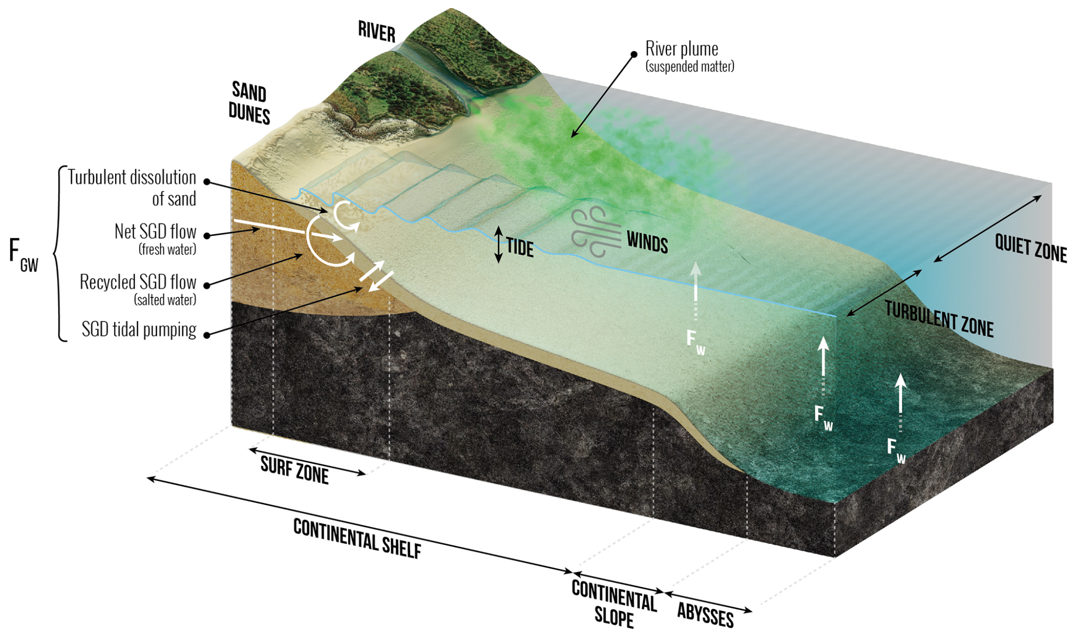

Figure 2. Schematic view of the low-temperature processes that control the dissolution of (either amorphous or crystallized) siliceous minerals in seawater in and to the coastal zone and in the deep ocean, feeding F_{GW} and F_W. These processes correspond to both low and medium energy flux dissipated per volume of a given siliceous particle in the coastal zone, in the continental margins, and in the abysses and to high-energy flux dissipated in the surf zone. Details are given in S1 in the Supplement.

stantial (e.g., Ehlert et al., 2016b). Focusing on processes occurring in tidal sands, Anschultz et al. (2009) showed that they can be a biogeochemical reactor for the Si cycle. Extrapolating laboratory-based dissolution experiments performed with pure quartz, Fabre et al. (2019) calculated the potential flux of dissolution of siliceous sandy beaches that is driven by wave and tidal action. If, according to Luijendijk et al. (2018) one-third of the world's shorelines are sandy beaches, this dissolution flux could be $3.2(\pm 1.0)$ Tmol Si yr^{-1}. However, this estimate is not well constrained because it has not been validated by field experiments (Sect. S2 in the Supplement). Cho et al. (2018), using a ^{228}Ra inverse model and groundwater dSi/^{228}Ra ratios, estimate the total (terrestrial + marine) SGD dSi flux to the ocean to be $3.8(\pm 1.0)$ Tmol Si yr^{-1}; this represents an upper limit value for SGD's contribution to the global ocean dSi cycle. Without systematic data that corroborate the net input of dSi through the circulation of the marine component of SGD (e.g., porewater δ^{30}Si, paired dSi and ^{228}Ra measurements), we estimate the range of net input of dSi through total SGD as 0.7 Tmol Si yr^{-1} (Rahman et al., 2019) to 3.8 Tmol Si yr^{-1} (Cho et al., 2018), with an average, i.e., $F_{GW} = 2.3(\pm 1.1)$ Tmol Si yr^{-1}, which is approximately 3 times larger than that of Tréguer and De La Rocha (2013).

2.4 (Sub)polar glaciers (F_{ISMW})

This flux was not considered by Tréguer and De La Rocha (2013). Several researchers have now identified polar glaciers as sources of Si to marine environments (Tréguer, 2014; Meire et al., 2016; Hawkings et al., 2017). The current best estimate of discharge-weighted dSi concentration in (sub)Arctic glacial meltwater rivers lies between 20–30 µM, although concentrations ranging between 3 and 425 µM have been reported (Graly et al., 2014; Meire et al., 2016; Hatton et al., 2019). Only two values currently exist for dSi from subglacial meltwater beneath the Antarctic Ice Sheet (Whillans subglacial lake and Mercer subglacial lake, 126–140 µM; Michaud et al., 2016, Hawkings et al., 2020), and there is a limited dataset from periphery glaciers in the McMurdo Dry Valleys and Antarctic Peninsula (≈ 10–120 µM; Hatton et al., 2020; Hirst et al., 2020). Furthermore, iceberg dSi concentrations remain poorly quantified but are expected to be low (≈ 5 µM; Meire et al., 2016). Meltwater typically contains high suspended sediment concentrations, due to intense physical erosion by glaciers, with a relatively high dissolvable aSi component (0.3 %–1.5 % dry weight) equating to concentrations of 70–340 µM (Hawkings et al., 2018; Hatton et al., 2019). Iceberg aSi concentrations are lower (28–83 µM) (Hawkings et al., 2017). This particulate phase appears fairly soluble in seawater (Hawkings et al., 2017), and large benthic dSi fluxes in glacially influenced shelf seas have been observed (Hendry et al., 2019; Ng et al., 2020). Direct silicic acid input from (sub)polar glaciers is estimated to be $0.04(\pm 0.04)$ Tmol Si yr^{-1}. If the aSi flux is considered then this may provide an additional $0.29(\pm 0.22)$ Tmol Si yr^{-1}, with a total F_{ISMW} (=

dSi + aSi) input estimate of $0.33(\pm 0.26)$ Tmol Si yr^{-1}. This does not include any additional flux from benthic processing of glacially derived particles in the coastal regions (see Sect. 2.2 above).

2.5 Hydrothermal activity (F_H)

The estimate of Tréguer and De La Rocha (2013) for F_H was $0.6(\pm 0.4)$ Tmol Si yr^{-1}. Seafloor hydrothermal activity at mid-ocean ridges (MORs) and ridge flanks is one of the fundamental processes controlling the exchange of heat and chemical species between seawater and ocean crust (Wheat and Mottl, 2000). A major challenge limiting our current models of both heat and mass flux (e.g., Si flux) through the seafloor is estimating the distribution of the various forms of hydrothermal fluxes, including focused (i.e., high temperature) vs. diffuse (i.e., low temperature) and ridge axis vs. ridge flank fluxes. Estimates of the Si flux for each input are detailed below.

Axial and near-axial hydrothermal flux settings. The best estimate of the heat flux at ridge axis (i.e., crust 0–0.1 Ma in age) is $1.8(\pm 0.4)$ TW, while the heat flux in the near-axial region (i.e., crust 0.1–1 Ma in age) has been inferred at $1.0(\pm 0.5)$ TW (Mottl, 2003). The conversion of heat flux to hydrothermal water and chemical fluxes requires assumptions regarding the temperature at which this heat is removed. For an exit temperature of $350(\pm 30)$ °C typical of black smoker vent fluids, and an associated enthalpy of $1500(\pm 190)$ J g^{-1} at 450–1000 bar and heat flux of $2.8(\pm 0.4)$ TW, the required seawater flux is $5.9(\pm 0.8) \times 10^{16}$ g yr^{-1} (Mottl, 2003). High-temperature hydrothermal dSi flux is calculated using a dSi concentration of $19(\pm 11)$ mmol kg^{-1}, which is the average concentration in hydrothermal vent fluids that have an exit temperature > 300 °C (Mottl, 2012). This estimate is based on a compilation of > 100 discrete vent fluid data, corrected for seawater mixing (i.e., end-member values at Mg = 0; Edmond et al., 1979) and phase separation. Although the chlorinity of hot springs varies widely, nearly all of the reacted fluid, whether vapor or brine, must eventually exit the crust within the axial region. The integrated hot spring flux must therefore have a chlorinity similar to that of seawater. The relatively large range of dSi concentrations in high-temperature hydrothermal fluids likely reflect the range of geological settings (e.g., fast- and slow-spreading ridges) and host-rock composition (ultramafic, basaltic, or felsic rocks). Because dSi enrichment in hydrothermal fluids results from mineral–fluid interactions at depth and is mainly controlled by the solubility of secondary minerals such as quartz (Mottl 1983; Von Damm et al. 1991), it is also possible to obtain a theoretical estimate of the concentration of dSi in global hydrothermal vent fluids. Under the conditions of temperature and pressure (i.e., depth) corresponding to the base of the upflow zone of high temperature (> 350–450 °C) hydrothermal systems, dSi concentrations between 16 and 22 mmol kg^{-1} are calculated, which is in good agreement with measured values in end-member hydrothermal fluids. Using a dSi concentration of $19(\pm 3.5)$ mmol kg^{-1} and water flux of $4.8(\pm 0.8) \times 10^{16}$ g yr^{-1}, we determine an axial hydrothermal Si flux of $0.91(\pm 0.29)$ Tmol Si yr^{-1}. It should be noted, however, that high-temperature hydrothermal fluids may not be entirely responsible for the transport of all the axial hydrothermal heat flux (Elderfield and Schultz, 1996; Nielsen et al., 2006). Because dSi concentrations in diffuse hydrothermal fluids are not significantly affected by subsurface Si precipitation during cooling of the hydrothermal fluid (Escoube et al., 2015), we propose that the global hydrothermal Si flux is not strongly controlled by the nature (focused vs. diffuse) of axial fluid flow.

Ridge flank hydrothermal fluxes. Chemical fluxes related to seawater–crust exchange at ridge flanks have been previously determined through direct monitoring of fluids from low-temperature hydrothermal circulation (Wheat and Mottl, 2000). Using basaltic formation fluids from the 3.5 Ma crust on the eastern flank of the Juan de Fuca Ridge (Wheat and McManus, 2005), a global flux of 0.011 Tmol Si yr^{-1} for the warm ridge flank is calculated. This estimate is based on the measured Si anomaly associated with warm spring (0.17 mmol kg^{-1}) and a ridge flank fluid flux determined using oceanic Mg mass balance, therefore assuming that the ocean is at steady state with respect to Mg. More recent results of basement fluid compositions in cold and oxygenated ridge flank settings (e.g., North Pond, Mid-Atlantic Ridge) also confirm that incipient alteration of volcanic rocks may result in significant release of Si to circulating seawater (Meyer et al., 2016). The total heat flux through ridge flanks, from 1 Ma crust to a sealing age of 65 Ma, has been estimated at $7.1(\pm 2)$ TW. Considering that most of ridge flank hydrothermal power output should occur at cool sites (< 20 °C), the flux of slightly altered seawater could range from 0.2 to 2×10^{19} g yr^{-1}, rivaling the flux of river water to the ocean of 3.8×10^{19} g yr^{-1} (Mottl, 2003). Using this estimate and Si anomaly of 0.07 mmol − Si kg^{-1} reported in cold ridge flank setting from North Pond (Meyer et al., 2016), a Si flux of 0.14 to 1.4 Tmol Si yr^{-1} for the cold ridge flank could be calculated. Because of the large volume of seawater interacting with oceanic basalts in ridge flank settings, even a small chemical anomaly resulting from reactions within these cold systems could result in a globally significant elemental flux. Hence, additional studies are required to better determine the importance of ridge flanks to oceanic Si budget.

Combining axial and ridge flank estimates, the best estimate for F_H is now $1.7(\pm 0.8)$ Tmol Si yr^{-1}, approximately 3 times larger than the estimate from Tréguer and De La Rocha (2013).

2.6 Total net inputs (Table 1A)

Total Si input $= 8.1(\pm 2.0)(F_{\mathrm{R(dSi+aSi)}}) + 0.5(\pm 0.5)(F_{\mathrm{A}}) + 1.9(\pm 0.7)(F_{\mathrm{W}}) + 2.3(\pm 1.1)(F_{\mathrm{GW}}) + 0.3(\pm 0.3)(F_{\mathrm{ISMW}}) + 1.7(\pm 0.8)(F_{\mathrm{H}}) = 14.8(\pm 2.6)$ Tmol Si yr^{-1}.

The uncertainty of the total Si inputs (and total Si outputs, Sect. 3) has been calculated using the error propagation method from Bevington and Robinson (2003). This has been done for both the total fluxes and the individual flux estimates.

3 Advances in output fluxes

3.1 Long-term burial of planktonic biogenic silica in sediments (F_{B})

Long-term burial of bSi, which generally occurs below the top 10–20 cm of sediment, was estimated by Tréguer and De La Rocha (2013) to be $6.3(\pm 3.6)$ Tmol Si yr^{-1}. The burial rates are highest in the Southern Ocean (SO), the North Pacific Ocean, the equatorial Pacific Ocean, and the coastal and continental margin zone (CCMZ; DeMaster, 2002; Hou et al., 2019; Rahman et al., 2017).

Post-depositional redistribution by processes like winnowing or focusing by bottom currents can lead to under- and over-estimation of uncorrected sedimentation and burial rates. To correct for these processes, the burial rates are typically normalized using the particle reactive nuclide ^{230}Th method (e.g., Geibert et al., 2005). A ^{230}Th normalization of bSi burial rates has been extensively used for the SO (Tréguer and De La Rocha, 2013), particularly in the "opal belt" zone (Pondaven et al., 2000; DeMaster, 2002; Geibert et al., 2005). Chase et al. (2015) re-estimated the SO burial flux, south of 40° S at $2.3(\pm 1.0)$ Tmol Si yr^{-1}.

Hayes et al. (2020, 2021) recently calculated total marine bSi burial of $5.46(\pm 1.18)$ Tmol Si yr^{-1}, using a database that comprises 2948 bSi concentrations of top core sediments and ^{230}Th-corrected accumulation fluxes of open-ocean locations $>$ 1 km in depth. The ^{230}Th-corrected total burial rate of Hayes et al. (2021) is $2.68(\pm 0.61)$ Tmol Si yr^{-1} south of 40° S, close to the estimate of Chase et al. (2015) for the SO. Hayes et al. (2021) do not distinguish between the different analytical methods used for the determination of the bSi concentrations of these 2948 samples to calculate total bSi burial. These methods include alkaline digestion methods (with variable protocols for correcting from lithogenic interferences; e.g., DeMaster, 1981; Mortlock and Froelich, 1989; Müller and Schneider, 1993), X-ray diffraction (e.g., Leinen et al., 1986), X-ray fluorescence (e.g., Finney et al., 1988), Fourier-transform infrared spectroscopy (Lippold et al., 2012), and inductively coupled plasma mass spectrometry (e.g., Prakash Babu et al., 2002). An international exercise calibration on the determination of bSi concentrations of various sediments (Conley, 1998) concluded that the X-ray diffraction (XRD) method generated bSi concentrations that were on average 24 % higher than the alkaline digestion methods. In order to test the influence of the XRD method on their re-estimate of total bSi burial, Hayes et al. (2021) found that their re-estimate ($5.46(\pm 1.18)$ Tmol Si yr^{-1}), which includes XRD data (≈ 40 % of the total number of data points), did not differ significantly from a re-estimate that does not include XRD data points ($5.43(\pm 1.18)$ Tmol Si yr^{-1}). As a result, this review includes the re-estimate of Hayes et al. (2021) for the open-ocean annual burial rate, i.e., $5.5(\pm 1.2)$ Tmol Si yr^{-1}.

The best estimate for the open-ocean total burial now becomes $2.8(\pm 0.6)$ Tmol Si yr^{-1} without the SO contribution ($2.7(\pm 0.6)$ Tmol Si yr^{-1}). This value is an excess of 1.8 Tmol Si yr^{-1} over the DeMaster (2002) and Tréguer and De La Rocha (2013) estimates, which were based on 31 sediment cores mainly distributed in the Bering Sea, the North Pacific, the Sea of Okhotsk, and the equatorial Pacific (total area 23 million square kilometers) and where bSi % was determined solely using alkaline digestion methods.

Estimates of the silica burial rates have usually been determined from carbon burial rates using a Si : C ratio of 0.6 in CCMZ (DeMaster 2002). However, we now have independent estimates of marine organic C and total initial bSi burial (e.g., Aller et al., 1996, 2008; Galy et al., 2007; Rahman et al., 2016, 2017). It has been shown that the initial bSi burial in sediment evolved as unaltered bSi or as authigenically formed aluminosilicate phases (Rahman et al., 2017). The Si : C burial ratios of residual marine plankton post-remineralization in tropical and subtropical deltaic systems are much greater (2.4–11) than the 0.6 Si : C burial ratio assumed for continental margin deposits (DeMaster, 2002). The sedimentary Si : C preservation ratios are therefore suggested to depend on differential remineralization pathways of marine bSi and C_{org} under different diagenetic regimes (Aller, 2014). Partitioning of ^{32}Si activities between bSi and mineral pools in tropical deltaic sediments indicate rapid and near-complete transformation of initially deposited bSi to authigenic clay phases (Rahman et al., 2017). For example, in subtropical/temperate deltaic and estuarine deposits, ^{32}Si activities represent approximately ≈ 50 % of initial bSi$_{\mathrm{opal}}$ delivery to sediments (Rahman et al., 2017). Using the ^{32}Si technique, Rahman et al. (2017) provided an updated estimate of bSi burial for the CCMZ of $3.7(\pm 2.1)$ Tmol Si yr^{-1}, higher than the Tréguer and De La Rocha (2013) estimate of $3.3(\pm 2.1)$ Tmol Si yr^{-1} based on the Si : C method of DeMaster (2002).

Combining the Hayes et al. (2021) burial rate for the open-ocean zone including the SO and the Rahman et al. (2017) estimate for the CCMZ gives a revised global total burial flux, F_{B}, of $9.2(\pm 1.6)$ Tmol Si yr^{-1}, 46 % larger than the Tréguer and De La Rocha (2013) estimate.

3.2 Deposition and long-term burial of sponge silica (F_{SP})

The estimate of Tréguer and De La Rocha (2013) for F_{SP}, the net sink of sponge bSi in sediments of continental margins, was $3.6(\pm 3.7)$ Tmol Si yr^{-1}. The longevity of sponges, ranging from years to millennia, temporally decouples the process of skeleton production from the process of deposition to the sediments (Jochum et al., 2017). While sponges slowly accumulate bSi over their long and variable lifetimes (depending on the species), the deposition to the sediments of the accumulated bSi is a relatively rapid process after sponge death, lasting days to months (Sect. S3 in the Supplement). The estimate of Tréguer and De La Rocha (2013) was calculated as the difference between the sponge dSi demand on continental shelves ($3.7(\pm 3.6)$ Tmol Si yr^{-1}) – estimated from silicon consumption rates available for a few sublittoral sponge species (Maldonado et al., 2011) – and the flux of dSi from the dissolution of sponge skeletons in continental shelves ($0.15(\pm 0.15)$ Tmol Si yr^{-1}). This flux was tentatively estimated from the rate of dSi dissolution from a rare, unique glass sponge reef in British Columbia (Canada; Chu et al., 2011) and which is unlikely to be representative of the portion of sponge bSi that dissolves back as dSi after sponge death and before their burial in the sediments. To improve the estimate, Maldonado et al. (2019) used microscopy to access the amount of sponge silica that was actually being buried in the marine sediments using 17 sediment cores representing different marine environments. The deposition of sponge bSi was found to be 1 order of magnitude more intense in sediments of continental margins and seamounts than on continental rises and central basin bottoms. The new best estimate for F_{SP} is $1.7(\pm 1.6)$ Tmol Si yr^{-1}, assuming that the rate of sponge silica deposition in each core was approximately constant through the Holocene, i.e., 2 times smaller than Tréguer and De La Rocha's preliminary estimate.

3.3 Reverse weathering flux (F_{RW})

The previous estimate for this output flux, provided by Tréguer and De La Rocha (2013), $F_{RW} = 1.5(\pm 0.5)$ Tmol Si yr^{-1}, was determined using indirect evidence since the influence of reverse weathering on the global Si cycle prior to 2013 was poorly understood. For example, reverse weathering reactions at the sediment–water interface were previously thought to constitute a relatively minor sink (0.03–0.6 Tmol Si yr^{-1}) of silica in the ocean (DeMaster, 1981). The transformation of bSi to a neoformed aluminosilicate phase, or authigenic clay formation, was assumed to proceed slowly ($> 10^4$–10^5 years) owing principally to the difficulty of distinguishing the contribution of background lithogenic or detrital clays using the common leachates employed to quantify bSi (DeMaster, 1981). Recent direct evidence supporting the rapid formation of authigenic clays comes from tropical and subtropical deltas (Michalopoulos and Aller, 1995; Rahman et al., 2016, 2017; Zhao et al., 2017), and several geochemical tools show that authigenic clays may form ubiquitously in the global ocean (Michalopoulos and Aller, 2004; Ehlert et al., 2016a; Baronas et al., 2017; Geilert et al., 2020; Pickering et al., 2020). Activities of cosmogenic ^{32}Si ($t_{1/2} \approx 140$ years), incorporated into bSi in the surface ocean, provide demonstrable proof of rapid reverse weathering reactions by tracking the fate of bSi upon delivery to marine sediments (Rahman et al., 2016). By differentiating sedimentary bSi storage between unaltered bSi (bSi_{opal}) and diagenetically altered bSi ($bSi_{altered}$) in the proximal coastal zone, ^{32}Si activities in these pools indicate that 3.7 Tmol Si yr^{-1} is buried as unaltered bSi_{opal} and $4.7(\pm 2.3)$ Tmol Si yr^{-1} as authigenic clays (bSi_{clay}) on a global scale. Here, we adopt 4.7 Tmol Si yr^{-1} for F_{RW} representing about 3 times the value of Tréguer and De La Rocha (2013).

3.4 Total net output (Table 1A)

Total Si output = 9.2 (± 1.6) (F_B(net deposit)) + 4.7 (± 2.3) (F_{RW}) + 1.7 (± 1.6) (F_{SP}) = 15.6 (± 2.4) Tmol Si yr^{-1}.

4 Advances in biological fluxes

4.1 Annual bSi pelagic production

4.1.1 From field data

The last evaluation of global marine silica production was by Nelson et al. (1995), who estimated global gross marine bSi pelagic production to be $240(\pm 40)$ Tmol Si yr^{-1}. Since 1995, the number of field studies of bSi production (using either the ^{30}Si tracer method, Nelson and Goering (1977), or the ^{32}Si method (Tréguer et al., 1991; Brzezinski and Phillips, 1997)) has grown substantially from 15 (1995) to 49 in 2019, allowing the first estimate based on empirical silica production rate measurements (Fig. 3 and Sect. S4 in the Supplement). It is usually assumed that the silica production, as measured using the above methods, is mostly supported by diatoms, with some unknown (but minor) contribution of other planktonic species.

The silica production rates measured during 49 field campaigns were assigned to Longhurst provinces (Longhurst, 2007; Longhurst et al., 1995) based on location, with the exception of the SO, where province boundaries were defined according to Tréguer and Jacques (1992). Extrapolating these "time-and-space-limited" measurements of bSi spatially to a biogeographic province, and annually from the bloom phenology for each province (calculated as the number of days where the chlorophyll concentration is greater than the average concentration between the maximum and the minimum values), results in annual silica production estimates for 26 of the 56 world ocean provinces. The annual production of all provinces in a basin were averaged for the "ocean basin" esti-

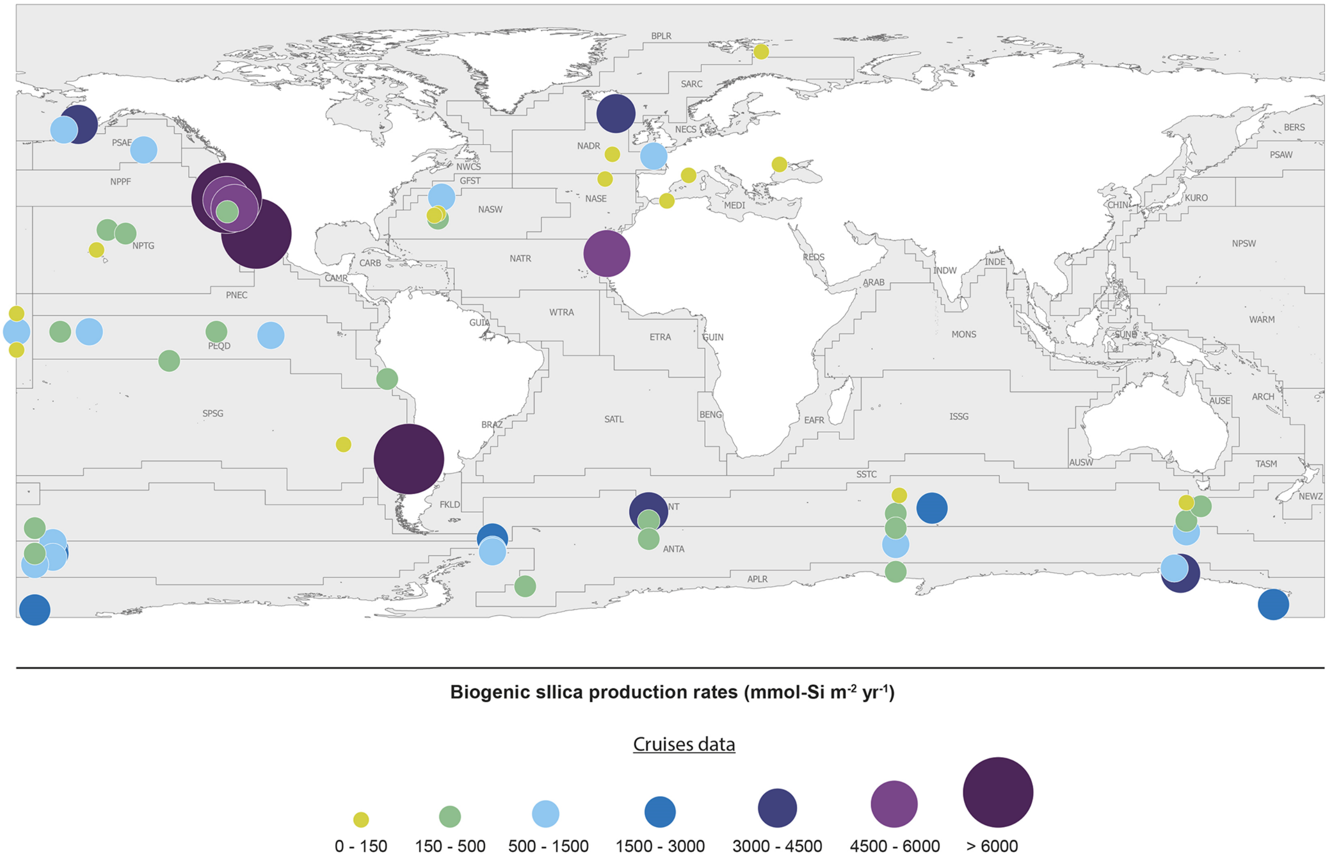

Figure 3. Biogenic silica production measurements in the world ocean. Distribution of stations in the Longhurst biogeochemical provinces (Longhurst, 2007; Longhurst et al., 1995). All data are shown in Sect. S4 in the Supplement (Annex 1).

mate (Table 2) and then extrapolated by basin area. The averages from provinces were subdivided among coastal for the "domain" estimate (Table 2), SO, and open-ocean domains and extrapolated based on the area of each domain. Averaging the ocean basin and the domain estimates (Table 2), our best estimate for the annual global marine bSi production is 267(±18) Tmol Si yr^{-1} (Table 2).

4.1.2 Annual bSi pelagic production from models

Estimates of bSi production were also derived from satellite productivity models and from global ocean biogeochemical models (GOBMs). We used global net primary production (NPP) estimates from the carbon-based productivity model (Westberry et al., 2008) and the vertically generalized productivity model (VGPM) (Behrenfeld and Falkowski, 1997) for the estimates based on satellite productivity models. NPP estimates from these models were divided into oligotrophic (< 0.1 µg chl a L^{-1}), mesotrophic (0.1–1.0 µg chl a L^{-1}), and eutrophic (> 1.0 µg chl a L^{-1}) areas (Carr et al., 2006). The fraction of productivity by diatoms in each area was determined using the DARWIN model (Dutkiewicz et al., 2015), allowing a global estimate where diatoms account for 29 % of the production. Each category was further subdivided into high-nutrient low-chlorophyll (HNLC) zones (> 5 µM surface nitrate; Garcia et al., 2014), coastal zones (< 300 km from a coastline), and open-ocean (remainder) zones for application of Si : C ratios to convert to diatom silica production. Si : C ratios were 0.52 for HNLC regions, 0.065 for the open ocean, and 0.13 for the coastal regions, reflecting the effect of Fe limitation in HNLC areas (Franck et al., 2000), of Si limitation for uptake in the open ocean (Brzezinski et al., 1998, 2011; Brzezinski and Nelson, 1996; Krause et al., 2012), and of replete conditions in the coastal zone (Brzezinski, 1985). Silica production estimates were then subdivided between coast (within 300 km of shore), open ocean, and SO (northern boundary 43° S from Australia to South America, 34.8° S from South America to Australia) and summed to produce regional estimates (Table 2). Our best estimate for the global marine bSi production is 207(±23) Tmol Si yr^{-1} from satellite productivity models (Table 2).

A second model-based estimate of silica production used 18 numerical GOBMs models of the marine silica cycle that all estimated global silica export from the surface ocean (Gnanadesikian and Toggweiler, 1999; Usbeck, 1999;

Table 1. Si inputs, outputs, and biological fluxes at word ocean scale.

A – Estimates for Si inputs and outputs			
Inputs	$Tmol\ Si\,yr^{-1}$	Reference	
$F_{R(dSi+aSi)}$ rivers	8.1(±2.0)	Tréguer and De La Rocha (2013); Frings et al. (2016)	
F_A aeolian	0.5(±0.5)	Tréguer and De La Rocha (2013)	
F_W dissolution lithogenic Si	1.9(±0.7)	Tréguer and De La Rocha (2013)	
F_{GW} submar. groundwater	2.3(±1.1)	Cho et al. (2018); Rahman et al. (2019); this review	
F_{ISMW} (sub)polar glaciers	0.3(±0.3)	This review	
F_H hydrothermal	1.7(±0.8)	This review	
Total input estimate	14.8(±2.6)		
Outputs	$Tmol\ Si\,yr^{-1}$	Reference	
F_B (net deposit) burial	9.2(±1.6)	This review, Hayes et al. (2021)	
F_{SP} sponges	1.7(±1.6)	Maldonado et al. (2019)	
F_{RW} reverse weathering	4.7(±2.3)	Rahman et al. (2016, 2017)	
Total outputs	15.6(±2.4)		
B – Comparative estimates of Si fluxes			
	Refs. (1) and (2)	This review	Difference (%)
Net inputs ($Tmol\ Si\,yr^{-1}$)	9.4(±4.7)	14.8(±2.6)	57 %
Net outputs ($Tmol\ Si\,yr^{-1}$)	11.4(±7.6)	15.6(±2.4)	37 %
Gross bSi pelag. prod. ($Tmol\ Si\,yr^{-1}$)	240(±40)	255(±52)	6 %
D:P (production: dissolution)	0.56	0.56	
τ_G residence time (kyr)	12.5 (3)	7.7	−38 %
τ_B residence time (kyr)	0.50 (3)	0.47	−6 %
$\tau_G : \tau_B$	25 (3)	16	−34 %

References are (1) Nelson et al. (1995) and (2) Tréguer and De La Rocha (2013). (3) Recalculated from our updated dSi inventory value; see Supplement for detailed definition of flux term (in detailed legend of Fig. 1).

Table 2. Biological fluxes (F_{Pgross} in $Tmol\ Si\,yr^{-1}$).

	World ocean	Coast	Southern Ocean	Open ocean
Silica production from models				
– Satellite productivity models	207(±23)	56(±18)	60(±12)	91(±2)
– Ocean biogeochemical models	276(±22)		129(±19)	
Average of models	242(±49)			
Silica production field studies				
– Ocean basin	249			
– Domain	285	138	67	80
Average of field studies	267(±18)			
Global estimate	255(±52)			

Global silica production as determined from numerical models and extrapolated from field measurements of silica production (uncertainties are standard errors).

Heinze et al., 2003; Wischmeyer et al., 2003; Jin et al., 2006; Dunne et al., 2007; Sarmiento et al., 2007; Bernard et al., 2011; Ward et al., 2012; Matsumoto et al., 2013; De Souza et al. 2014; Holzer et al., 2014; Aumont et al., 2015; Dutkiewicz et al., 2015; Pasquier and Holzer, 2017; Roshan et al., 2018). These include variants of the MOM, HAMOCC OCIM, DARWIN, cGENIE, and PICES models. Export production was converted to gross silica production by using a silica dissolution-to-production (D : P) ratio for the surface open ocean of 0.58 and 0.51 for the surface of coastal regions (Tréguer and De La Rocha, 2013). Model results were first averaged within variants of the same model and then averaged across models to eliminate biassing the average to any particular model. Our best estimate from GOBMs for the global marine bSi production is $276(\pm 23)$ Tmol Si yr^{-1} (Table 2). Averaging the estimates calculated from satellite productivity models and GOBMs gives a value of $242(\pm 49)$ Tmol Si yr^{-1} for the global marine bSi production (Table 2).

4.1.3 Best estimate for annual bSi pelagic production

Using a simple average of the "field" and "model" estimates, the revised best estimate of global marine gross bSi production, mostly due to diatoms, is now $F_{\mathrm{Pgross}} = 255(\pm 52)$ Tmol Si yr^{-1}, not significantly different from the Nelson et al. (1995) value.

In the SO, a key area for the world ocean Si cycle (DeMaster, 1981), there is some disagreement among the different methods of estimating bSi production. Field studies give an estimate of 67 Tmol Si yr^{-1} for the annual gross production of silica in the SO, close to the estimate of 60 Tmol Si yr^{-1} calculated using satellite productivity models (Table 2). However, the bSi production in the SO estimated by ocean biogeochemical models is about twice as high, at 129 Tmol Si yr^{-1} (Table 2). The existing in situ bSi production estimates are too sparse to be able to definitively settle whether the lower estimate or the higher estimate is correct, but there is reason to believe that there are potential biases in both the satellite NPP models and the ocean biogeochemical models. SO chlorophyll concentrations may be underestimated by as much as a factor of 3–4 (Johnson et al., 2013), which affects the NPP estimates in this region and hence our bSi production estimates with this method. The bSi production estimated by ocean biogeochemical models is highly sensitive to vertical exchange rates in the SO (Gnanadesikan and Toggweiler, 1999) and is also dependent on the representation of phytoplankton classes in models with explicit representation of phytoplankton. Models that have excessive vertical exchange in the SO (Gnanadesikan and Toggweiler, 1999), or that represent all large phytoplankton as diatoms, may overestimate the Si uptake by plankton in the SO. Other sources of uncertainty in our bSi production estimates include poorly constrained estimates of the Si : C ratio and dissolution-to-production ratios (see Sect. S4 in the Supplement). The errors incurred by these choices are more likely to cancel out in the global average but could be significant at regional scales, potentially contributing to the discrepancies in SO productivity across the various methods.

4.1.4 Estimates of the bSi production of other pelagic organisms

Extrapolations from field and laboratory work show that the contribution of picocyanobacteria (like *Synechococcus*; Baines et al. 2012, Brzezinski et al., 2017; Krause et al., 2017) to the world ocean accumulation of bSi is $<$ 20 Tmol Si yr^{-1}. The gross silica production of rhizarians, siliceous protists, in the 0–1000 m layer might range between 2–58 Tmol Si yr^{-1}, about 50 % of it occurring in the 0–200 m layer (Llopis Monferrer et al., 2020).

Note that these preliminary estimates of bSi accumulation or production by picocyanobacteria and rhizarians are within the uncertainty of our best estimate of F_{Pgross}.

4.2 Estimates of the bSi production of benthic organisms

The above-updated estimate of the pelagic production does not take into account bSi production by benthic organisms like benthic diatoms and sponges. Our knowledge of the production terms for benthic diatoms is poor, and no robust estimate is available for bSi annual production of benthic diatoms at a global scale (Sect. S4 in the Supplement).

Substantial progress has been made for silica deposition by siliceous sponges recently. Laboratory and field studies reveal that sponges are highly inefficient in the molecular transport of dSi compared to diatoms and consequently bSi production, particularly when dSi concentrations are lower than 75 µM, a situation that applies to most ocean areas (Maldonado et al., 2020). On average, sponge communities are known to produce bSi at rates that are about 2 orders of magnitude smaller than those measured for diatom communities (Maldonado et al., 2012). The global standing crop of sponges is very difficult to be constrained. The annual bSi production attained by such standing crop is even more difficult to estimate because sponge populations are not homogeneously distributed on the marine benthic environment, and extensive, poorly mapped, and unquantified aggregations of heavily silicified sponges occur in the deep sea of all oceans. A first tentative estimate of bSi production for sponges on continental shelves, where sponge biomass can be more easily approximated, ranged widely, from 0.87 to 7.39 Tmol Si yr^{-1}, because of persisting uncertainties in estimating sponge standing crop (Maldonado et al., 2012). A way to estimate the global annual bSi production by sponges without knowing their standing crop is to retrace bSi production values from the amount of sponge bSi that is annually being deposited to the ocean bottom, after assuming that, in the long run, the standing crop of sponges in the ocean is in equilibrium (i.e it is neither progressively increasing nor decreasing over time). The deposition rate of sponge bSi has been estimated at $49.95(\pm 74.14)$ mmol−Si m^{-2} yr^{-1} on continental margins, at $0.44(\pm 0.37)$ mmol − Si m^{-2} yr^{-1} in sediments of ocean basins where sponge aggregations do not occur, and at $127.30(\pm 105.69)$ mmol − Si m^{-2} yr^{-1} in deep-water sponge aggregations (Maldonado et al., 2019). A corrected sponge bSi deposition rate for ocean basins is estimated at $2.98(\pm 1.86)$ mmol − Si m^{-2} yr^{-1} assuming that sponge aggregations do not occupy more than 2 % of seafloor of ocean basins (Maldonado et al., 2019). A total value of $6.15(\pm 5.86)$ Tmol Si yr^{-1} can be estimated for the global ocean when the average sponge bSi deposition rate for continental margins and seamounts (representing 108.02 million squarekilometers of seafloor) and for ocean basins (253.86 million squarekilometers) is scaled up through the extension of those bottom compartments. If the bSi production being accumulated as standing stock in the living sponge populations annually is assumed to become constant in a long-term equilibrium state, the global annual deposition rate of sponge bSi can be considered a reliable estimate of the minimum value that the annual bSi production by the sponges can reach in the global ocean. The large associated SD value does not derive from the approach being unreliable but from the spatial distribution of the sponges on the marine bottom being extremely heterogeneous, with some ocean areas being very rich in sponges and sponge bSi in sediments at different spatial scales while other areas are completely deprived of these organisms.

5 Discussion

5.1 Overall residence times

The overall geological residence time for Si in the ocean (τ_G) is equal to the total amount of dSi in the ocean divided by the net input (or output) flux. We re-estimate the total ocean dSi inventory value derived from the Pandora model (Peng et al. 1993), which according to Tréguer et al. (1995) was 97 000 Tmol Si. An updated estimate of the global marine dSi inventory was computed by interpolating the objectively analyzed annual mean silicate concentrations from the 2018 World Ocean Atlas (Garcia et al., 2019) to the OCIM model grid (Roshan et al., 2018). Our estimate is now 120 000 Tmol Si, i.e., about 24 % higher than the Tréguer et al. (1995) estimate. Tables 1B and 3 show updated estimates of τ_G from Tréguer et al. (1995) and Tréguer and De La Rocha (2013) using this updated estimate of the total dSi inventory. Our updated budget (Fig. 1, Tables 1B and 3A) reduces past estimates of τ_G (Tréguer et al., 1995; Tréguer and De La Rocha, 2013) by more than half, from ca. 18 kyr to ca. 8 kyr (Table 3C). This brings the ocean residence time of Si closer to that of nitrogen (< 3 kyr; Sarmiento and Gruber, 2006) than phosphorus (30–50 kyr; Sarmiento and Gruber, 2006).

The overall biological residence time, τ_B, is calculated by dividing the total dSi content of the world ocean by gross silica production. It is calculated from the bSi pelagic production only given the large uncertainty on our estimate of the bSi production by sponges. τ_B is ca. 470 years (Tables 1B and 3). Thus, Si delivered to the ocean passes through the biological uptake and dissolution cycle on average 16 times (τ_G/τ_B) before being removed to the sea floor (Tables 1B and 3C).

The new estimate for the global average preservation efficiency of bSi buried in sediments is ($F_B/F_{Pgross} =$ $(9.2/255) =$) 3.6 %, which is similar to the Tréguer and De La Rocha (2013) estimate. This makes bSi in sediments an intriguing potential proxy for export production (Tréguer et al., 2018). Note that the reverse weathering flux (F_{RW}) is also fed by the export flux (F_E) (Fig. 4). So, the preservation ratio of biogenic silica in sediment can be calculated as $(F_B + F_{RW})/F_{Pgross} = (13.9/255) = 5.45\,\%$, which is ≈ 30 times larger than the carbon preservation efficiency.

5.2 The issue of steady state

Over a given timescale, an elemental cycle is at steady state if the outputs balance the inputs in the ocean and the mean concentration of the dissolved element remains constant.

5.2.1 Long timescales (> τ_G)

Over geologic timescales, the average dSi concentration of the ocean has undergone drastic changes. A seminal work (Siever, 1991) on the biological–geochemical interplay of the Si cycle showed a decline of a factor of 100 in ocean dSi concentration from 550 Myr ago to the present. This decline was marked by the rise of silicifiers like radiolarian and sponges during the Phanerozoic. Then during the mid-Cenozoic diatoms started to dominate a Si cycle previously controlled by inorganic and diagenetic processes. Conley et al. (2017) hypothesized that biological processes might also have influenced the dSi concentration of the ocean at the start of oxygenic photosynthesis, taking into account the impact of the evolution of biosilicifying organisms (including bacteria-related metabolism). There is further evidence that the existing lineages of sponges have their origin in ancient (Mesozoic) oceans with much higher dSi concentrations than the modern ocean. Some recent sponge species can only complete their silica skeletons if dSi concentration much higher than that in their natural habitat is provided experimentally (Maldonado et al., 1999). Also, all recent sponge species investigated to date have kinetics of dSi consumption that reach their maximum speed only at dSi concentrations that are 1 to 2 orders of magnitude higher than the current dSi availability in the sponge habitats, indicating that the sponge physiology evolved in dSi-richer ancestral scenarios. Note that with a geological residence time of Si of ca. 8000 years, the Si cycle can fluctuate over glacial–interglacial timescales.

5.2.2 Short timescales (< τ_G)

In the modern ocean the main control over silica burial and authigenic formation rate is the bSi production rate of pelagic and benthic silicifiers, as shown above. The gross production of bSi due to diatoms depends on the dSi availability in the surface layer (Fig. 1). Silicic acid does not appear to be limiting in several zones of the world ocean, which include the coastal zones and the HNLC zones (Tréguer and De La Rocha, 2013). Note that any short-term change of dSi inputs does not imply modification of bSi production, or ex-

Table 3. A total of 25 years of evolution of the estimates for Si inputs, outputs, biological production, and residence times at World Ocean scale.

A – Estimates for Si input and output fluxes			
References	(1)	(2)	(3)
Inputs (Tmol Si yr^{-1})			
$F_{R(dSi+aSi)}$ rivers	5.0(±1.1)	7.3(±2.0)	8.1(±2.0)
F_A aeolian	0.5(±0.5)	0.5(±0.5)	0.5(±0.5)
F_W dissolution lithogenic silica	0.4(±0.3)	1.9(±0.7)	1.9(±0.7)
F_{GW} submar. groundwater	–	0.6(±0.6)	2.3(±1.1)
F_{ISMW} (sub)polar glaciers	–	–	0.3(±0.3)
F_H hydrothermal	0.2(±0.1)	0.6(±0.4)	1.7(±0.8)
Total input estimate	6.1(±2.0)	9.4(±4.7)	14.8(±2.6)
Outputs (Tmol Si yr^{-1})			
$F_{B(net\ deposit)}$ burial	7.1(±1.8)	6.3(±3.6)	9.2(±1.6)
F_{SP} sponges	–	3.6(±3.7)	1.7(±1.6)
F_{RW} reverse weathering	–	1.5(±0.5)	4.7(±2.3)
Total output estimate	7.1(±1.8)	11.4(±7.6)	15.6(±2.4)
B – Estimates for gross production of biogenic silica (Tmol Si yr^{-1})			
References	(4)	(3)	
Gross production of biogenic silica	240(±40)	255(±52)	
C – Residence time of Si (kyr)			
References	(1)	(2)	(3)
τ_G residence time (geological)	18.3[(5)]	12.5[(5)]	7.7
τ_B residence time (biological)	0.50[(5)]	0.50[(5)]	0.47
$\tau_G : \tau_B$	37[(5)]	25[(5)]	16

References are as follows. (1) Tréguer et al. (1995). (2) Tréguer and De La Rocha (2013). (3) This review. (4) Nelson et al. (1995). [(5)] Recalculated from our updated dSi inventory value.

port or burial rate. For this reason, climatic changes or anthropogenic impacts that affect dSi inputs to the ocean by rivers and/or other pathways could lead to an imbalance of Si inputs and outputs in the modern ocean.

5.2.3 A possible steady-state scenario

Within the limits of uncertainty, the total net inputs of dSi and aSi are 14.8(±2.6) Tmol Si yr^{-1} and are approximately balanced by the total net output flux of Si of 15.6(±2.4) Tmol Si yr^{-1}. Figure 1 supports the hypothesis that the modern ocean Si cycle is at steady state, compatible with the geochemical and biological fluxes of Table 1.

Consistent with Fig. 1, Fig. 4 shows a steady-state scenario for the Si cycle in the coastal and continental margin zone (CCMZ), often called the "boundary exchange" zone which, according to Jeandel (2016) and Jeandel and Oelkers (2015), plays a major role in the land-to-ocean transfer of material (also see Fig. 2). Figure 4 illustrates the interconnection between geochemical and biological Si fluxes, particularly in the CCMZ. In agreement with Laruelle et al. (2009), Fig. 4 also shows that the open-ocean bSi production is mostly fueled by dSi inputs from below (92.5 Tmol Si yr^{-1}) and not by the CCMZ (4.7 Tmol Si yr^{-1}) (Sect. S5 in the Supplement).

5.3 The impacts of global change on the Si cycle

As illustrated by Figs. 1 and 4, the pelagic bSi production is mostly fueled from the large recycled deep-ocean pool of dSi. This lengthens the response time of the Si cycle to changes in dSi inputs to the ocean due to global change (including climatic and anthropogenic effects), increasing the possibility for the Si cycle to be out of balance.

5.3.1 Impacts on riverine inputs of dSi and aSi

Climate change at short timescales during the 21st century impacts the ocean delivery of riverine inputs of dSi and aSi (F_R) and of the terrestrial component of the submarine groundwater discharge (F_{GW}), either directly (e.g., dSi and aSi weathering and transport) or indirectly by affecting forestry and agricultural dSi export. So far the impacts of climate change on the terrestrial Si cycle have been reported for boreal wetlands (Struyf et al., 2010), North American (Opalinka and Cowling, 2015) and western Canadian Arc-

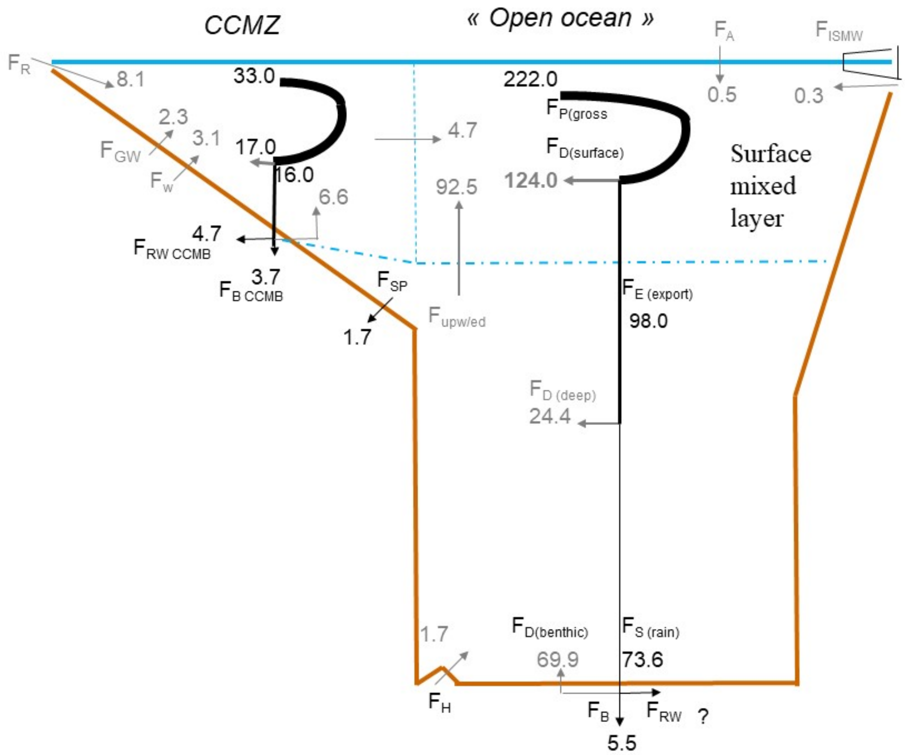

Figure 4. Schematic view of the Si cycle in the coastal and continental margin zone (CCMZ), linked to the rest of the world ocean (open-ocean zone, including upwelling and polar zones). In this steady-state scenario, consistent with Fig. 1, total inputs = total outputs = 15.6 Tmol Si yr^{-1}. This figure illustrates the links between biological, burial, and reverse weathering fluxes. It also shows that the open-ocean bSi (pelagic) production ($F_{P(gross)}$ = 222 Tmol Si yr^{-1}) is mostly fueled by dSi inputs from below 92.5 Tmol Si yr^{-1}, with the CCMZ only providing 4.7 Tmol Si yr^{-1} to the open ocean.

tic rivers (Phillips, 2020), and the tributaries of the Laptev and East Siberian seas (Charette et al., 2020), but not for tropical environments. Tropical watersheds are the key areas for the transfer of terrestrial dSi to the ocean, as approximately 74 % of the riverine Si input is from these regions (Tréguer et al., 1995). Precipitation in tropical regions usually follows the "rich-get-richer" mechanism in a warming climate according to model predictions (Chou et al., 2004, 2008). In other words, in tropical convergence zones rainfall increases with climatological precipitation, but the opposite is true in tropical subsidence regions, creating diverging impacts for the weathering of tropical soils. If predictions of global temperature increase and variations in precipitations of the IPCC are correct (IPCC, 2018), it is uncertain how F_R or F_{GW}, two major components of dSi and aSi inputs, will change. Consistent with these considerations are the conclusions of Phillips (2020) on the impacts of climate change on the riverine delivery of dSi to the ocean, using a machine-learning-based approach. Phillips (2020) predicts that within the end of this century dSi mean yield could increase regionally (for instance in the Arctic region), but the global mean dSi yield is projected to decrease, using a model based on 30 environmental variables including temperature, precipitation, land cover, lithology, and terrain.

5.3.2 Abundance of marine and pelagic and benthic silicifiers

A change in diatom abundance was not seen on the North Atlantic from continuous plankton recorder (CPR) data over the period 1960–2009 (Hinder et al., 2012). However, studies have cautioned that many fields (e.g., chl) will take several decades before these changes can be measured precisely beyond natural variability (Henson et al 2010; Dutkiewicz et al 2019). The melting of Antarctic ice platforms has already been noticed to trigger impressive population blooms of highly silicified sponges (Fillinger et al., 2013).

5.3.3 Predictions for the ocean phytoplankton production and bSi production

Climate change in the 21st century will affect ocean circulation, stratification, and upwelling and therefore nutrient cycling (Aumont et al., 2003; Bopp et al., 2005, 2013). With increased stratification, dSi supply from upwelling will decrease (Figs. 1 and 4), leading to less siliceous phytoplankton production in surface compartments of lower latitudes and possibly the North Atlantic (Tréguer et al., 2018). The impact of climate change on the phytoplankton production in polar seas is highly debated as melting of sea ice decreases light limitation. In the Arctic Ocean an increase in nutrient supply from river- and shelf-derived waters (at the least for silicic acid) will occur through the Transpolar Drift, potentially impacting rates of primary production, including bSi production (e.g., Charette et al., 2020). In the SO bSi production may increase in the coastal and continental shelf zone as iron availability increases due to ice sheet melt and iceberg delivery (Duprat et al., 2016; Boyd et al., 2016; Herraiz-Borreguero et al., 2016; Hutchins and Boyd, 2016; Tréguer et al., 2018; Hawkings et al., in press). However, Henley et al. (2019) suggest a shift from diatoms to haptophytes and cryptophytes with changes in ice coverage in the western Antarctic Peninsula. How such changes in coastal environments and nutrient supplies will interplay is unknown. Globally, it is very likely that a warmer and more acidic ocean alters the pelagic bSi production rates, thus modifying the export production and outputs of Si at short timescales.

Although uncertainty is substantial, modeling studies (Bopp et al., 2005; Laufkötter et al., 2015; Dutkiewicz et al., 2019) suggest regional shifts in bSi pelagic production with climatic change. These models predict a global decrease in diatom biomass and productivity over the 21st century (Bopp et al., 2005, Laufkötter et al., 2015; Dutkiewicz et al., 2019), which would lead to a reduction in the pelagic biological flux of silica. Regional responses differ, with most models suggesting a decrease in diatom productivity in the lower latitudes and many predicting an increase in diatom productivity in the SO (Laufkötter et al., 2015). Holzer et al. (2014) suggest that changes in supply of dissolved iron (dFe) will alter bSi production mainly by inducing floristic shifts, not by relieving kinetic limitation. Increased primary productivity is predicted to come from a reduction in sea ice area, faster growth rates in warmer waters, and longer growing seasons in the high latitudes. However, many models have very simple ecosystems including only diatoms and small phytoplankton. In these models, increased primary production in the SO is mostly from diatoms. Models with more complex ecosystem representations (i.e., including additional phytoplankton groups) suggest that increased primary productivity in the future SO will be due to other phytoplankton types (e.g., pico-eukaryote) and that diatoms' biomass will decrease (Dutkiewicz et al., 2019; also see model PlankTOM5.3 in Laufkötter et al., 2015), except in regions where sea ice cover has decreased. Differences in the complexity of the ecosystem and parameterizations, in particular in terms of temperature dependences of biological process, between models lead to widely varying predictions (Laufkotter et al., 2015; Dutkiewicz et al., 2019). These uncertainties suggest we should be cautious in our predictions of what will happen with the silica biogeochemical cycle in a future ocean.

5.4 Other anthropogenic impacts

For decades if not centuries, anthropogenic activities directly or indirectly altered the Si cycle in rivers and the CCMZ (Conley et al., 1993; Ittekot et al., 2000, 2006; Derry et al., 2005; Humborg et al., 2006; Laruelle et al., 2009; Bernard et al., 2010; Liu et al., 2012; Yang et al., 2015; Wang et al., 2018a; Zhang et al., 2019). Processes involved include eutrophication and pollution (Conley et al., 1993; Liu et al., 2012), river damming (Ittekot et al., 2000; Ittekot et al., 2006; Yang et al., 2015; Wang et al., 2018), deforestation (Conley et al., 2008), changes in weathering and in river discharge (Bernard et al., 2010; Yang et al., 2015), and deposition load in river deltas (Yang et al., 2015).

Among these processes, river damming is known for having the most spectacular and short-timescale impacts on the Si delivery to the ocean. River damming favors enhanced biologically mediated absorption of dSi in the dam reservoir, thus resulting in significant decreases in dSi concentration downstream. Drastic perturbations in the Si cycle and downstream ecosystem have been shown (Ittekot et al., 2000; Humborg et al., 2006; Ittekot, 2006; Zhang et al., 2019), particularly downstream of the Nile (Mediterranean Sea), the Danube (Black Sea), and the fluvial system of the Baltic Sea. Damming is a critical issue for major rivers of the tropical zone (Amazon, Congo, Changjiang, Huanghe, Ganges, Brahmaputra, etc.), which carry 74 % of the global exorheic dSi flux (Tréguer et al., 1995; Dürr et al., 2011). Among these major rivers, the course of the Amazon and Congo is, so far, not affected by a dam or, as for the Congo River, the consequence of Congo damming for the Si cycle in the equatorial African coastal system has not been studied. The case of Changjiang (Yangtze), one of the major world players in dSi delivery to the ocean, is of particular interest. Interestingly, the Changjiang (Yangtze) River dSi concentrations decreased dramatically from the 1960s to 2000 (before the building of the Three Gorges Dam, TGD). This decrease is attributed to a combination of natural and anthropogenic impacts (Wang et al., 2018a). Paradoxically, since the construction of the TGD (2006–2009) no evidence of additional retention of dSi by the dam has been demonstrated (Wang et al., 2018a).

Over the 21st century, the influence of climate change, and other anthropogenic modifications, will have variable impacts on the regional and global biogeochemical cycling of Si. The input of dSi will likely increase in specific regions (e.g., Arctic Ocean), whilst inputs to the global ocean might decrease. Global warming will increase stratification of the surface ocean, leading to a decrease in dSi inputs from the deep sea, although this is unlikely to influence the Southern Ocean (see Sect. 5.3.3). Model-based predictions suggest a global decrease in diatom production, with a subsequent decrease in export production and Si burial rate. Clearly, new observations are needed to validate model predictions.

6 Conclusions and recommendations

The main question that still needs to be addressed is whether the contemporary marine Si cycle is at steady state, which requires the uncertainty in total inputs and outputs to be minimized.

For the input fluxes, more effort is required to quantify groundwater input fluxes, particularly using geochemical techniques to identify the recycled marine flux from other processes that generate a net input of dSi to the ocean. In light of laboratory experiments by Fabre et al. (2019) demonstrating low-temperature dissolution of quartz in clastic sand beaches, collective multinational effort should examine whether sandy beaches are major global dSi sources to the ocean. Studies addressing uncertainties at the regional scale are critically needed. Further, better constraints on hydrothermal inputs (for the northeast Pacific-specific case), aeolian input, and subsequent dissolution of minerals both in the coastal and in open-ocean zones and inputs from ice melt in polar regions are required.

For the output fluxes, it is clear that the alkaline digestion of biogenic silica (DeMaster, 1981; Mortlock and Froelich, 1989, Müller and Schneider, 1993), one of the commonly used methods for bSi determination in sediments, is not always effective at digesting all the bSi present in sediments. This is especially true for highly silicified diatom frustules, radiolarian tests, or sponge spicules (Maldonado et al., 2019; Pickering et al., 2020). Quantitative determination of bSi is particularly difficult for lithogenic or silicate-rich sediments (e.g., estuarine and coastal zones), for example those of the Chinese seas. An analytical effort for the quantitative determination of bSi from a variety of sediment sources and the organization of an international comparative analytical exercise are of high priority for future research. It is also clear that reverse weathering processes are important not only in estuarine or coastal environments, but also in distal coastal zones, slope, and open-ocean regions of the global ocean (Michalopoulos and Aller, 2014; Chong et al., 2016; Ehlert et al., 2016a; Baronas et al., 2017; Geilert et al., 2020; Pickering et al., 2020). Careful use of geochemical tools (e.g., ^{32}Si, Ge/Si, δ^{30}Si: Ehlert et al., 2016; Ng et al., 2020; Geilert et al., 2020; Pickering et al., 2020; Cassarino et al., in press) to trace partitioning of bSi between opal and authigenic clay phases may further elucidate the magnitude of this sink, particularly in understudied areas of the ocean.

This review highlights the significant progress that has been made in the past decade toward improving our quantitative and qualitative understanding of the sources, sinks, and internal fluxes of the marine Si cycle. Filling the knowledge gaps identified in this review is also essential if we are to anticipate changes in the Si cycle, and their ecological and biogeochemical impacts, in the future ocean.

Data availability. All data used in this review article are available in the referenced articles. Data of biogenic pelagic production are shown in the Supplement (Annex 1).

Supplement. The supplement related to this article is available online at: https://doi.org/10.5194/bg-18-1269-2021-supplement.

Author contributions. PJT and JNS defined the manuscript content and wrote the paper. MAC, CE, JH, SR, OR, and PT wrote the input section. JS, CE, SR, and MM wrote the output section. MB, TD, SD, AL, and PT wrote the pelagic production section. MLA and MM wrote the sponge subsections. SML, LR, and PT wrote the discussion section. Every author re-read and approved the review article.

Competing interests. The authors declare that they have no conflict of interest.

Acknowledgements. The idea for this paper was conceived during a conference of the SILICAMICS Network, held in June 2018 at the University of Victoria (Canada). Thanks are due to Sébastien Hervé (LEMAR-IUEM, Plouzané) for his artwork.

Financial support. This work was supported by the French National Research Agency (18-CEO1-0011-01) and by the Spanish Ministry of Science, Innovation and Universities (PID2019-108627RB-I00).

Review statement. This paper was edited by Emilio Marañón and reviewed by two anonymous referees.

References

Aller, R. C.: Sedimentary diagenesis, depositional environments, and benthic fluxes, in: Treatise on Geochemistry: Second edition, edited by: Holland, H. D. and Turekian, K. K., Elsevier, Oxford, 8, 293–334, 2014.

Aller, R. C., Blair, N. E., and Brunskill, G. J.: Early diagenetic cycling, incineration, and burial of sedimentary organic carbon in the central Gulf of Papua (Papua New Guinea), J. Geophys. Res. Earth Surf., 113, 1–22, 2008.

Aller, R. C., Blair, N. E., Xia, Q., and Rude, P. D.: Remineralization rates, recycling, and storage of carbon in Amazon shelf sediments, Cont. Shelf Res., 16, 753–786, 1996.

Anschutz, P., Smith, T., Mouret, A., Deborde, J., Bujan, S., Poirier, D., and Lecroart, P.: Tidal sands as biogeochemical reactors, Estuar. Coast. Shelf Sci., 84, 84–90, 2009.

Arsouze, T., Dutay, J.-C., Lacan, F., and Jeandel, C.: Reconstructing the Nd oceanic cycle using a coupled dynamical – biogeochemical model, Biogeosciences, 6, 2829–2846, https://doi.org/10.5194/bg-6-2829-2009, 2009.

Aumont, O., Maier-Reimer, E., Blain, S., and Monfray, P.: An ecosystem model of the global ocean including Fe, Si, P co-limitations, Global Biogeochem. Cycles, 17, 1060, https://doi.org/10.1029/2001GB001745, 2003.

Aumont, O., Ethé, C., Tagliabue, A., Bopp, L., and Gehlen, M.: PISCES-v2: an ocean biogeochemical model for carbon and ecosystem studies, Geosci. Model Dev., 8, 2465–2513, https://doi.org/10.5194/gmd-8-2465-2015, 2015.

Baines, S. B., Twining, B. S., Brzezinski, M. A., Krause, J. W., Vogt, S., Assael, D., and McDaniel, H.: Significant silicon accumulation by marine picocyanobacteria, Nat. Geosci., 5, 886–891, 2012.

Baronas, J. J., Hammond, D. E., McManus, J., Wheat, C. G., and Siebert, C. A.: Global Ge isotope budget, Geochim. Cosmochim. Acta, 203, 265–83, 2017.

Beck, A. J., Charette, M. A., Cochran, J. K., Gonneea, M. E., Peucker-Ehrenbrink, B.: Dissolved strontium in the subterranean estuary – Implications for the marine strontium isotope budget, Geochim. Cosmochim. Acta., 117, 33–52, 2013.

Behrenfeld, M. J. and Falkowski, P. G.: Photosynthetic rates derived from satellite-based chlorophyll concentration, Limnol. Oceanogr., 42, 1–20, 1997.

Bernard, C. Y., Laruelle, G. G., Slomp, C. P., and Heinze, C.: Impact of changes in river fluxes of silica on the global marine silicon cycle: a model comparison, Biogeosciences, 7, 441–453, https://doi.org/10.5194/bg-7-441-2010, 2010.

Bernard, C. Y., Dürr, H. H., Heinze, C., Segschneider, J., and Maier-Reimer, E.: Contribution of riverine nutrients to the silicon biogeochemistry of the global ocean – a model study, Biogeosciences, 8, 551–564, https://doi.org/10.5194/bg-8-551-2011, 2011.

Berner, R. A., Lasaga, A. C., and Garrels, R. M.: The carbonate-silicate geochemical cycle and its effect on atmospheric carbon dioxide over the past 100 millions years, Am. J. Sci., 283, 641–683, 1983.

Bevington, P. R. and Robinson, D. K.: Data Reduction and Error Analysis for the Physical Sciences, third ed., McGrawHill, NewYork, 2003.

Bopp, L., Aumont, O., Cadule, P., Alvain, S., and Gehlen, G.: Response of diatoms distribution to global warming and potential implications: A global model study, Geophys. Res. Lett., 32, L19606, 2005.

Bopp, L., Resplandy, L., Orr, J. C., Doney, S. C., Dunne, J. P., Gehlen, M., Halloran, P., Heinze, C., Ilyina, T., Séférian, R., Tjiputra, J., and Vichi, M.: Multiple stressors of ocean ecosystems in the 21st century: projections with CMIP5 models, Biogeosciences, 10, 6225–6245, https://doi.org/10.5194/bg-10-6225-2013, 2013.

Boyd, P. W., Cornwall, C. E., Davison, A., Doney, S. C., Fourquez, M., Hurd, C. L., Lima, I. D., McMinn, A.: Biological responses to environmental heterogeneity under future ocean conditions, Glob. Change Biol., 22, 2633–2650, 2016.

Brzezinski, M. A.: The Si : C : N ratio of marine diatoms: Interspecific variability and the effect of some environmental variables, J. Phycol., 21, 347–357, 1985.

Brzezinski, M. A. and Nelson, D. M.: Chronic substrate limitation of silicic acid uptake rates in the western Sargasso Sea, Deep Sea Res. Part II Top. Stud. Oceanogr., 43, 437–453, 1996.

Brzezinski, M. A. and Phillips, D. R.: Evaluation of ^{32}Si as a tracer for measuring silica production rates in marine waters, Limnol. Oceanogr., 42, 856–865, 1997.

Brzezinski, M. A., Villareal, T. A., and Lipschultz, F.: Silica production and the contribution of diatoms to new and primary production in the central North Pacific, Mar. Ecol. Prog. Ser., 167, 89–104, 1998.

Brzezinski, M. A., Baines, S. B., Balch, W. M., Beucher, C. P., Chai, F., Dugdale, R. C., Krause, J. W., Landry, M. R., Marchi, A., Measures, C. I., Nelson, D. M., Parker, A. E., Poulton, A. J., Selph, K. E., Strutton, P. G., Taylor, A. G., and Twining, B. S.: Twining, Co-limitation of diatoms by iron and silicic acid in the equatorial Pacific, Deep Sea Res. Part II Top. Stud. Oceanogr., 58, 493–511, 2011.

Brzezinski, M. A., Krause, J. W., Baines, S. B., Collier, J. L., Ohnemus, D. C., and Twining, B. S.: Patterns and regulation of silicon accumulation in *Synechococcus* spp., J. Phycol., 53, 746–761, 2017.

Carr, M., Friedrichs, A. M., Schmeltz, M., Aita, M. N, Antoine, A., Arrigo, K. R., Asanuma, I, Aumont, O, Barber, R., Behrenfeld, M., Bidigare, R., Buitenhuis, E. T., Campbell, J., Ciotti, A., Dierssen, H., Dowell, M., Dunne, J., Esaias, W., Gentili, B., Gregg, W., Groom S., Hoepffner, N., Ishizakas, J., Kameda, T., Le Quéré, C., Lohren, S., Marra, J., Mélin, F., Moore, K., Morel, A., Reddy, T. E., Ryan, J., Scardi, M., Smyth, T., Turpie, K., Tilstone, G., Waters, K., and Tamanaka, Y.: A comparison of global estimates of marine primary production from ocean color, Deep Sea Res. Part II Top. Stud. Oceanogr., 53, 741–770, 2006.

Cassarino, L., Hendry, K. R., Henley, S. F., MacDonald, E., Arndt, S., Freitas, F. S., Pike, J., and Firing, Y. L.: Sedimentary nutrient supply in productive hot spots off the West Antarctic Peninsula revealed by silicon isotopes. Global Biogeochemical Cycles, 34, 1–17, e2019GB006486, https://doi.org/10.1029/2019GB006486, 2020.

Charette M. A., Kipp, L. E., Jensen, L. T., Dabrowski, J. S., Whitmore, L. M., Fitzsimmons, J. N., Williford, T., Ulfsbo, A., Jones, E., and Bundy, R. : The Transpolar Drift as a Source of Riverine and Shelf-Derived Trace Elements to the Central Arctic Ocean, J. Geophys. Res. Oceans, 125, e2019JC015920, https://doi.org/10.1029/2019jc015920, 2020.

Chase, Z., Kohfeld, K. E., and Matsumoto, K.: Controls on biogenic silica burial in the Southern Ocean, Global Biogeochem. Cycles, 29, 1599–1616, 2015.

Cho, H.-M., Kim, G., Kwon, E. Y., Moosdorf, N., Garcia-Orellana, J., and Santos, I. R.: Radium tracing nutrient inputs through submarine groundwater discharge in the global ocean, Sci. Rep., 8, 2439, 2018.

Chong, L. S., Berelson, W., Hammond, D. E., Fleisher, M. Q., Anderson, R. F., Rollins, N. E., and Lund, S.: Biogenic sedimentation and geochemical properties of deep-sea sediments of the Demerara slope/abyssal Plain: Influence of the Amazon River Plume, Mar. Geol., 379, 124–139, 2016.

Chou, C. and Neelin, J. D.: Mechanisms of global warming impacts on regional tropical precipitations, J. Clim., 17, 2688–2701, 2004.

Chou, C., Neelin, J. D., Chen, C.-A., and Tu, J.-Y.: Evaluating the "rich-get-richer" mechanism in tropical precipitation change under global warming, J. Clim., 22, 1982–2005, 2008.

Chu, J. W. F., Maldonado, M., Yahel, G., and Leys, S. P.: Glass sponge reefs as a silicon sink, Mar. Ecol. Progr. Series, 441, 1–14, https://doi.org/10.3354/meps09381, 2011.

Conley, D. J.: An interlaboratory comparison for the measurement of biogenic silica in sediments , Mar. Chem., 63, 39–48, 1998.

Conley, D. J., Schelske, C. L., and Stoermer, E. F.: Modification of the biogeochemical of silica with eutrophication, Mar. Ecol. Prog. Ser., 101, 179–192, 1993.

Conley, D. J, Likens, G. E., Buso, D. C., Saccone, L., Bailey, S. W., and Johnson, C. E.: Deforestation causes increased dissolved silicate losses in the Hubboard Brook Experimental Forest, Glob. Change Biol., 14, 2458–2554, 2008.

Conley, D. J., Frings, P. J., Fontorbe, G., Clymans, W., Stadmark, J., Hendry, K. R., Marron, A. O., and De La Rocha, C. L.: Biosilicification drives a decline of dissolved Si in the oceans through geologic time, Front. Mar. Sci., 4, 397, 2017.

De Souza, G. F., Slater, R. D., Dunne, J. P., and Sarmiento, J. L.: Deconvolving the controls on the deep ocean's silicon stable isotope distribution, Earth Planet. Sci. Lett., 398, 66–76, 2014.

DeMaster, D. J.: The supply and accumulation of silica in the marine environment, Geochim. Cosmochim. Acta, 45, 1715–1732, 1981.

DeMaster, D. J.: The accumulation and cycling of biogenic silica in the Southern Ocean: revisiting the marine silica budget, Deep Sea Res. Part II Top. Stud. Oceanogr., 49, 3155–3167, 2002.

Derry, L. A., Kurtz, A. C., Ziegler, K., and Chadwick, O. A.: Biological control of terrestrial silica cycling and export fluxes to watershed, Nature, 433, 728–731, 2005.

Dunne, J. P., Sarmiento, J. L., and Gnanadesikan, A.: A synthesis of global particle export from the surface ocean and cycling through the ocean interior and on the seafloor, Global Biogeochem. Cycles, 21, GB4006, 2007.

Duprat, L. P. A. M., Bigg, G. R., and Winton, D. J.: Enhanced Southern Ocean marine productivity due to fertilization by giant icebergs, Nat. Geosci., 9, 219–221, 2016.

Dürr, H. H., Meybeck, M., Hartmann, J., Laruelle, G. G., and Roubeix, V.: Global spatial distribution of natural riverine silica inputs to the coastal zone, Biogeosciences, 8, 597–620, https://doi.org/10.5194/bg-8-597-2011, 2011.

Dutkiewicz, S., Hickman, A. E., Jahn, O., Gregg, W. W., Mouw, C. B., and Follows, M. J.: Capturing optically important constituents and properties in a marine biogeochemical and ecosystem model, Biogeosciences, 12, 4447–4481, https://doi.org/10.5194/bg-12-4447-2015, 2015.

Dutkiewicz, S., Hickman, E., Jahn, O., Henson, S., Beaulieu, B. and Monier, E.: Ocean colour signature of climate change, Nat. Commun., 10, 019, 2019.

Edmond, J. M., Measures, C., Mangum, B., Grant, B., F. R. Sclater, F. R., Collier, R, Hudson, A., Gordon, L. I., and Corliss, J. B.: On the formation of metal-rich deposits at ridge crests, Earth. Planet. Sci. Lett., 46, 19–30, 1979.

Ehlert, C., Doeringa, K. Wallmanna, K., Scholza, F., Sommera, S., Grasse, P., Geilert, S., and Frank, M.: Stable silicon isotope signatures of marine pore waters – Biogenic opal dissolution versus authigenic clay mineral formation, Geochim. Cosmochim. Acta, 191, 102–117, 2016a.

Ehlert, C., Reckhardt, A., Greskowiak, J., Liguori, B. T. P., Böning, P., Paffratha, R., Brumsack, H.-J., and Pahnkea, K.: Transformation of silicon in a sandy beach ecosystem: insights from stable silicon isotopes from fresh and saline groundwaters, Chem. Geol., 440, 207–218, 2016b.

Elderfield, H. and Schultz, A.: Mid-ocean ridge hydrothermal fluxes and the chemical composition of the ocean, Annu. Rev. Earth Planet. Sci., 24, 191–224, 1996.

Escoube, R., Rouxel, O., Edwards, K., Glazer, B., and Donard, O.: Coupled Ge/Si and Ge isotope ratios as geochemical tracers of seafloor hydrothermal systems: case studies at Loihi Seamount and East Pacific Rise 9°50' N. Geochim. Cosmochim. Acta, 167, 93–112, 2015.

Fabre, S., Jeandel, C., Zambardi, T., Roustan, M., and Almar, R.: An overlooked silica source of the modern oceans: are sandy beaches the key?, Front. Earth Sci., 7, 231, 2019.

Fillinger, L., Janussen, D., Lundälv, T., and Richter, C.: Rapid glass sponge expansion after climate-induced Antarctic ice shelf collapse, Curr. Biol., 23, 1330–1334, 2013.

Finney, B. P., Lyle, M. W., and Heath, G. R.: Sedimentation at MANOP Site H (eastern equatorial Pacific) over the past 400 000 years: Climatically induced redox variations and their effects on transition metal cycling, Paleoceanography, 3, 169–189, https://doi.org/10.1029/PA003i002p00169, 1988.

Franck, V. M., Brzezinski, M. A., Coale, K. H., and Nelson, D. M.: Iron and silicic acid concentrations regulate Si uptake north and south of the Polar Frontal Zone in the Pacific Sector of the Southern Ocean, Deep. Res. Part II Top. Stud. Oceanogr., 47, 3315–3338, 2000.

Frings, P.: Revisiting the dissolution of biogenic Si in marine sediments: a key term in the ocean Si budget, Acta Geochim, 36, 429–432, 2017.

Frings, P. J., Clymans, W., Fontorbe, G., De La Rocha, C. L., and Conley, D. J.: The continental Si cycle and its impact on the ocean Si isotope budget, Chem. Geol., 425, 12–36, 2016.

Galy, V. C., France-Lanord, C., Beysac, O., Faure, P., Kudrass, H., and Pahol, F.: Efficient organic carbon burial in the Bengal fan sustained by the Himalayan erosional system, Nature, 450, 407–410, 2007.

Garcia, H. E., Locarnini, R. A., Boyer, T. P., Antonov, J. I., Baranova, O. K., Zweng, M. M., and Reagan, J. R., and Johnson, D. R.: Dissolved Inorganic Nutrients (phosphate, nitrate, silicate), in: World Ocean Atlas 2013, edited by Levitus, Mishonov A., NOAA Atlas NESDIS 76, 25 pp., 2014.

Garcia, H. E., Weathers, K. W., Paver, C. R., Smolyar, I., Boyer, T. P., Locarnini, M. M., Zweng, M. M., Mishonov, A. V., Baranova, O. K., Seidov, D., Reagan, J. R.: World Ocean Atlas 2018, Vol. 4: Dissolved Inorganic Nutrients (phosphate, nitrate and nitrate+nitrite, silicate), A. Mishonov Technical Editor, NOAA Atlas NESDIS 84, 35 pp., 2019.

Geibert, W., Rutgers van der Loeff, M. M., Usbeck, R., Gersonde, R., Kuhn, G., and Seeberg-Elverfeldt, J.: Quantifying the opal belt in the Atlantic and southeast Pacific sector of the Southern Ocean by means of ^{230}Th normalization, Global Biogeochem. Cycles, 19, GB4001, 2005.

Geilert, S., Grasse, P., Wallmann, K., Liebetrau, V., and Menzies, C. D.: Serpentine alteration as source of high dissolved silicon and elevated δ^{30}Si values to the marine Si cycle, Nat. Commun., 11, 1–10, https://doi.org/10.1038/s41467-020-18804-y, 2020.

Georg, R. B., West, A. J., Basu, A. R., and Halliday, A. N.: Silicon fluxes and isotope composition of direct groundwater discharge into the Bay of Bengal and the effect on the global ocean silicon isotope budget, Earth Planet. Sci. Lett., 203, 67–74, 2009.

Gnanadesikan, A. and Toggweiler, J. R.: Constraints placed by silicon cycling on vertical exchange in general circulation models, Geophys. Res. Lett., 26, 1865–1868, 1999.

Graly, J. A., Humphrey, N. F., Landowski, C. M., and Tarper, J. T.: Chemical weathering under the Greenland Ice Sheet, Geology, 42, 551–554, 2014.

Hatton, J. E., Hendry, K. R., Hawkings, J. R., Wadham, J. L., Kohler, T. J., Stibal, M., Beaton, A. D., Bagshaw, E. A., and Telling, J.: Investigation of subglacial weathering under the Greenland Ice Sheet using silicon isotopes, Geochim. Cosmochim. Acta, 247, 191–206, 2019.

Hatton, J. E., Hendry, K. R., Hirst, C., Opfergelt, S., Henkel, S., Silva-Busso, A., Welch, S. A., Wadham, J. L., Lyons, W. B., Bagsaw, E., Staubwasser, M., and McKgnight, D.: Silicon Isotopic Composition of Dry and Wet-Based Glaciers in Antarctica, Frontiers Earth Sci., 8, 11, 1–20, https://doi.org/10.3389/feart.2020.00286, 2020.

Hawkings, J. R., Wadham, J. L., Benning, L. G., Hendry, K. R., Tranter, M., Tedstone, A., Nienow, P., and Raiswell, R.: Ice sheets as a missing source of silica to the polar oceans, Nat. Commun., 8, 14198, 2017.

Hawkings, J. R., Hatton, J. E., Hendry, K. R., de Souza, G. F., Wadham, J. L., Ivanovic, R., Kohler, T. J., Stibal, M., Beaton, A., Lamarche-Gagnon, G., Tedstone, A., Hain, M. P., Bagshaw, E., Pike, J., and Tranter, M.: The silicon cycle impacted by past ice sheets, Nat. Commun., 9, 3210, 2018.

Hawkings, J. R., Skidmore, M. L., Wadham, J. L., Priscu, J. C., Morton, P. L., Hatton, J. E., Gardner, C. B., Kohler, T. J., Stibal, M., Bagshaw, E. A., Steigmeyer, A., Barker, J., Dore, J. E., Lyons, W. B., Tranter, M., and Spencer, R. G. M.: Enhanced trace element mobilization by the Earth's ice sheets, P. Natl. Acad. Sci. USA, 117, 31648–31659, https://doi.org/10.1073/pnas.2014378117, 2020.

Hayes, C. T., Costa, K., Calvo, E., Chase, Z., Demina, L. L., Dutay, J.-C., German, C. R., Heimbürger-Boavida, L.-E., Jaccard, S. L., Jacobel, A. W., Kohfeld, K. E., Kravchishina, M. D., Lippold, J., Mekik, F., Missiaen, L., Pavia, F. J., Paytan, A., Pedrosa-Pamies, R., Petrova, M. V., Rahman, S., Robinson, L. F., Roy-Barman, M., Sanchez-Vidal, A., Shiller, A., Tagliabue, A., Tessin, A. C., van Hulten, M., Zhang, J.-W.: Global Ocean Seafloor Sediment Geochemistry Data during the past 12,000 years, NOAA Paleoclimatology Data Center, available at: https://www.ncdc.noaa.gov/paleo-search/study/30512, last access: 21 July 2020.

Hayes, C. T., Costa, K. M., Anderson, R. F., Calvo, E., Chase Z., Demina L. L., Dutay, J.-C., German, C. R., Heimbürger-Boavida, L.-E., Jaccard, S. L., Jacob, A., Kohfeld, K. E., Kravchishina, M. D., Lippold, J., Mekik, F., Missiaen, L., Pavia, F. J., Paytan, A., Pamies, Pedrosa-Pamies, R., Petrova, M. V., Rahman, S., Robinson L. F., Roy-Barman, M., Sanchez-Vidal, A., Shiller, A., Tagliabue, A., Tessin, A. C., van Hulten, M., and Zhang J.: Global ocean sediment composition and burial flux in the deep sea, Global Ocean Sediment Composition and Burial Flux in the Deep Sea, Earth and Space Science Ocean Archive, 41 pp., https://doi.org/10.1002/essoar.10506119.1, 2021.

Heinze, C., Hupe, A., Maier-Reimer, E., Dittert, N., and Ragueneau, O.: Sensitivity of the marine biospheric Si cycle for biogeochemical parameter variations, Global Biogeochem. Cycles, 17, 1086, https://doi.org/10.1029/2002GB001943, 2003.

Hendry, K. R., Huvenne, V. A.I, Robinson, L. F., Annett, A., Badger, M., Jacobel, A.W, Ng, H. C., Opher, J., Pickering, R. A., Taylor, M. L., Bates, S. L., Cooper, Z., Cusham, G. G., Goodwin, C., Hoy, S., Rowland, G., Samperiz, A., Williams, J. A., and Woodward, M. S.: The biogeochemical impact of glacial meltwater from Southwest Greenland, Prog. Oceanogr., 76, 102126, https://doi.org/10.1016/j.pocean.2019.102126, 2019.

Henley, S. F., Schofield, O. M., Hendry, K. R., Schloss, I. R., Steinberg, D.K, Moffath, C., Peck, L. S., Costa, D. P., Bakker, D. C. E., Hughes, C., Rozema, P. D., Ducklow, H. W., Abele, D., Stefels, J., Van Leeuwe, M. A., Brussaard, C. P. D., Buma, A. G. J., Kohu, J., Sahade, R., Friedlaender, A. S., Stammerjohn, S. E., Venables, H. J., and Meredith, M. P.: Variability and change in the west Antarctic Peninsula marine system: Research priorities and opportunities, Progr. Oceanogr., 173, 208–237, 2019.

Henson, S. A., Sarmiento, J. L., Dunne, J. P., Bopp, L., Lima, I., Doney, S. C., John, J., and Beaulieu, C.: Detection of anthropogenic climate change in satellite records of ocean chlorophyll and productivity, Biogeosciences, 7, 621–640, https://doi.org/10.5194/bg-7-621-2010, 2010.

Herraiz-Borreguero, L., Lannuzel, D., van der Merwe, P., Treverrow, A., and Pedro, J. B.: Large flux of iron from the Amery Ice Shelf marine ice to Prydz Bay, East Antarctica, J. Geophys. Res. Oceans, 121, 6009–6020, 2016.

Hinder, S. L., Hays, G. C., Edwards, M., Roberts, E. C., Walne, A. W., and Gravenor, M. B.: Changes in marine dinoflagellate and diatom abundance under climate change, Nat. Clim. Change, 2, 271–275, 2012.

Hirst, C., Opfergelt, S., Gaspard, F., Hendry, K. R., Hatton, J. E., Welch, S., McKnight, D. M., and Lyons, W. B.: Silicon Isotopes Reveal a Non-glacial Source of Silicon to Crescent Stream, McMurdo Dry Valleys, Antarctica, Front. Earth Sci., 8, 1–18, https://doi.org/10.3389/feart.2020.00229, 2020.

Holzer, M., Primeau, F. W., DeVries, T., and Matear, R.: The Southern Ocean silicon trap: Data-constrained estimates of regenerated silicic acid, trapping efficiencies, and global transport paths, J. Geophys. Res. Ocean, 119, 313–33, 2014.

Hou Y., Hammond, D. E., Berelson, W. M., Kemnitz, N., Adkins, J. F., and Lunstrum, A.: Spatial patterns of benthic silica flux in the North Pacific reflect upper ocean production, Deep Sea Res. Part I Oceanogr. Res. Pap., 148, 25–33, 2019.

Humborg C., Pastuszak, M., Aigars, J., H. Siegmund, H., Mörth, C.-M., and Ittekkot, V.: Decreased silica land-sea fluxes trough damming in the Baltic Sea catchment – significance of particle trapping and hydrological alteration, Biogeochemistry, 77, 265–281, 2006.

Hutchins, D. A. and Boyd, P. W.: Marine phytoplankton and the changing ocean iron cycle, Nat. Clim. Change, 6, 1072–1076, 2016.

IPCC: Summary for Policymakers of IPCC Special Report on Global Warming of 1.5 °C approved by government, available at: https://www.ipcc.ch/2018/10/08/summary-for-policymakers-of-ipcc-special-report-on-global-warming-of-1-5c-approved-by-governments/, 2018.

Ittekkot, V, Humborg C, and Schäfer P.: Hydrological alternations and marine biogeochemistry: a silicate issue?, Bioscience, 50, 776–82, 2000.

Ittekot, V.,Unger, D., Humborg, C., and Tac An, N. T. (Eds): The Silicon Cycle: Human Perturbations and Impacts on Aquatic Systems, Comm. Probl. Environ. (SCOPE) Ser. Vol. 66, Island Press, Washington, DC, 296 pp, 2006.

Jeandel, C.: Overview of the mechanisms that could explain the 'Boundary Exchange' at the land–ocean contact, Philos. Trans. Royal Soc. A, 374, 20150287, 2016.

Jeandel, C. and Oelkers, E. H.: The influence of terrigeneous particulate material dissolution on ocean chemistry and global elements cycles, Chem. Geol., 395, 50–56, 2015.

Jeandel, C., Peucker-Ehrenbrink B., Jones, M. T., Pearce, C. R., Oelkers, E. H., Godderis, Y., Lacan, F., Aumont, O., and Arsouze, T.: Ocean margins : the missing term for oceanic element budgets?, Eos, Trans. AGU, 92, 217, 2011.

Jin, X., Gruber, N. Dunne, J. P., Sarmiento, J. L., and Armstrong R. A.: Diagnosing the contribution of phytoplankton functional groups to the production and export of particulate organic carbon, $CaCO_3$, and opal from global nutrient and alkalinity distributions, Global Biogeochem. Cycles, 20, GB2015, 2006.

Jochum, K. P., Schuessler, J. A., Wang, X.-H., Stoll, B., Weis, U., Müller, W. E. G., Haug, G. H., Andreae, M. O., and Froelich, P. N.: Whole-ocean changes in silica and Ge/Si ratios during the last deglacial deduced from long-lived giant glass sponges, Geophys. Res. Lett., 44, 555–564, 2017.

Johnson, R., Strutton, P. G., Wright, S. W., McMinn, A., and Meiner, K. M.: Three improved satellite chlorophyll algorithms for the Southern Ocean, J. Geophys. Res. Oceans, 118, 3694–3703, https://doi.org/10.1002/jgrc.20270, 2013.

Jones, M., Pearce, C. R., and Oelkers, E. H.: An experimental study of the interaction of basaltic riverine particulate material and seawater, Geochim. Cosmochim. Acta, 77, 108–120, 2012.

Krause, J. W., Brzezinski, M. A., Villareal, T. A., and Wilson, W.: Increased kinetic efficiency for silicic acid uptake as a driver of summer diatom blooms in the North Pacific subtropical gyre, Limnol. Oceanogr., 57, 1084–1098, 2012.

Krause, J. W., Mark A. Brzezinski, M. A., Baines, S. B., Collier, J. L., Twining, B. S., Ohnemus, D. C.: Picoplankton contribution to biogenic silica stocks and production rates in the Sargasso Sea, Global Biogeochem. Cycles, 31, 762–774, 2017.

Laruelle, G. G., Roubeix, V., Sferratore, A., Brodherr, B., Ciuffa, D., Conley, D. J., Dürr, H. H., Garnier, J., Lancelot, Le Thi Phuong, Q., Meunier, J.-D., Meybeck, M., Michalopoulos, P., Moriceau, B., Ní Longphuirt, S., Loucaides, S., Papush, L., Presti, M., Ragueneau, O., Regnier, P. A. G., Saccone, L., Slomp, C. P., , Spiteri, C., and Van Cappelle, P.: Anthopogenic perturbations of the silicon cycle at the global scale: key role of the land-ocean transition, Global Biogeochem. Cycles, 23, GB4031, 1–17, 2009.

Laufkötter, C., Vogt, M., Gruber, N., Aita-Noguchi, M., Aumont, O., Bopp, L., Buitenhuis, E., Doney, S. C., Dunne, J., Hashioka, T., Hauck, J., Hirata, T., John, J., Le Quéré, C., Lima, I. D., Nakano, H., Seferian, R., Totterdell, I., Vichi, M., and Völker, C.: Drivers and uncertainties of future global marine primary production in marine ecosystem models, Biogeosciences, 12, 6955–6984, https://doi.org/10.5194/bg-12-6955-2015, 2015.

Leinen, M., Cwienk, D., Heath, G. R., Biscaye, P. E., Kolla, V., Thiede, J., and Dauphin, J. P.: Distribution of biogenic silica and quartz in recent deep-sea sediments, Geology, 14, 199–203, 1986

Li, L, Barry, D. A., Stagnitti, F., and Parlange, J. Y.: Submarine groundwater discharge and associated chemical input to a coastal sea, Water Resour. Res., 35, 3253–3259, 1999.

Lippold, J., Luo, Y., Francois, R., Allen, S. E., Gherardi, J., Pichat, S., Hickey, B., and Schulz, H.: Strength and geometry of the glacial Atlantic Meridional Overturning Circulation, Nat. Geosci., 5, 813–816, 2012.

Liu, S. M., Li, L. W., Zhang, G., Liu, Z., Yu, Z., and Ren, J. L.: Impacts of human activities on nutrient transports in the Huanghe (Yellow River) Estuary, J. Hydrol., 430–431, 103–110, 2012.

Llopis Monferrer, N., Boltovskoy, D., Tréguer, P., Méndez Sandin, M., Not, F., and Leynaert, A.: Estimating biogenic silica production of Rhizaria in the global ocean, Global Biogeochem. Cycles, 34, e2019GB006286, 2020.

Longhurst, A. R. (Ed.): Ecological Geography of the Sea, Academic Press, London, 2nd ed., 2007.

Longhurst, A., S. Sathyendranath, T. Platt, and Caverhill, C.: An estimate of global primary production in the ocean from satellite radiometer data, J. Plankton Res., 17, 1245–1271, 1995.

Luijendijk, A., Hagenaars, G., Roshanka, R., Baart, F., Donchyts, G., and Aarninkhof, S.: The state of the world's beaches, Sci. Rep., 8, 6641, 2018.

Maldonado M., Navarro L., Grasa A., Gonzalez A., and Vaquerizo I.: Silicon uptake by sponges: a twist to understanding nutrient cycling on continental margins, Sci. Rep., 1, 30, 2011.

Maldonado, M., Ribes, M., and van Duyl, F. C.: Nutrient fluxes through sponges, Adv. Mar. Biol., 62, 113–182, 2012.

Maldonado, M., López-Acosta, M., Sitjà, C., García-Puig, M., Galobart, C.,Ercilla, G., Leynaert, A.: Sponge skeletons as an important sink of silicon in the global oceans, Nat. Geosci. 12, 815–822, 2019.

Maldonado, M., López-Acosta, M., Beazley, L., Kenchington, E., Koutsouveli, V., and Riesgo, A.: Cooperation between passive and active silicon transporters clarifies the ecophysiology and evolution of biosilicification in sponges, Sci. Adv., 6, 1–14, https://doi.org/10.1126/sciadv.aba9322, 2020.

Matsumoto, K., Tokos, K., Huston, A., and Joy-Warren, H.: MESMO 2: a mechanistic marine silica cycle and coupling to a simple terrestrial scheme, Geosci. Model Dev., 6, 477–494, https://doi.org/10.5194/gmd-6-477-2013, 2013.

Meire, L., Meire, P., Struyf, E., Krawczyk, D. W., Arendt, K. E., Yde, J. C., Pedersen, T. J., Hopwood, M. J., Rysgaard, S., and Meysman, F. J. R.: High export of dissolve silica from the Greenland Ice Sheet, Geophys. Res. Lett. 43, 9173–9182, 2016.

Meyer, J. L., Jaekel, U., Tully, B. J., Glazer, B. T., Wheat, C. G., Lin, H.-T., Hsieh, C.-C., Cowen, J. P., Hulme, S. M., Girguis, P. R., and Huber, J. A.: A distinct and active bacterial community in cold oxygenated fluids circulating beneath the western flank of the Mid-Atlantic ridge, Sci. Rep., 6, 22541, 2016.

Michalopoulos, P. and Aller, R. C.: Rapid Clay Mineral Formation in Amazon Delta Sediments: Reverse Weathering and Oceanic Elemental Cycles, Science, 270, 614–617, 1995.

Michalopoulos, P. and Aller, R. C.: Early diagenesis of biogenic silica in the Amazon delta: alteration, authigenic clay formation, and storage, Geochim. Cosmochim. Acta, 68, 1061–1085, 2004.

Michaud, A. B., Skidmore, M. L., Mitchell, A. C., Vick-Majors, T. J., Barbante, C., Turetta, C., VanGelder, W., and Priscu, J. C.: Solute sources and geochemical processes in Subglacial Lake Whillans, West Antarctica, Geology, 44, 347–350, 2016.

Moriceau, B, Gehlen, M., Tréguer, P., Baines, S., Livage, J., and André, L.: Editorial: Biogeochemistry and genomics of silicification and silicifiers, Front. Mar. Sci. 6, 57, 2019.

Morin, G. P., Vigier, N., and Verney-Carronc, A.: Enhanced dissolution of basaltic glass in brackish waters: Impact on biogeochemical cycles, Earth Planet. Sci. Lett., 417, 1–8, 2015.

Mortlock, R. A. and Froelich, P. N.: A simple method for the rapid determination of biogenic opal in pelagic marine sediments, Deep Sea Res. Part I Oceanogr. Res. Pap., 36, 1415–1426, 1989.

Mottl, M. J.: Explanatory notes and master chemical item spreadsheet for the VentDB Data collections housed in the EarthChem Library, Version 1.0. Interdisciplinary Earth Data Alliance (IEDA), https://doi.org/10.1594/IEDA/100207, 2012.

Mottl, M. J.: Hydrothermal processes at seafloor spreading Centers: application of basalt-seawater experimental results, in: Rona, P. A., Boström, K., Laubier, L., and Smith, K. L. (eds) Hydrothermal Processes at Seafloor Spreading Centers. NATO Conference Series (IV Marine Sciences), 12. Springer, Boston, MA, https://doi.org/10.1007/978-1-4899-0402-7_10, 1983.

Mottl, M. J.: Partitioning of energy and mass fluxes between mid-ocean ridge axes and flanks at high and low temperature, in: Energy and Mass Transfer in Marine Hydrothermal Systems, edited by Halbach, P. E., Tunnicliffe, V., and Hein, J. R., Dahlem University Press, 271–286, 2003.

Müller, J. and Schneider, R.: An automated leaching method for the determination of opal in sediments and particulate matter, Deep Sea Res. Part I Oceanogr. Res. Pap., 40, 425–444, 1993.

Nelson, D. M. and Goering, J. J.: Near-surface silica dissolution in the upwelling region off northwest Africa, Deep Sea Res., 24, 65–73, 1977.

Nelson, D. M., Tréguer, P., Brzezinski, M. A., Leynaert, A., and Quéguiner, B.: Production and dissolution of biogenic silica in the ocean – Revised global estimates, comparison with regional data and relationship to biogenic sedimentation, Global Biogeochem. Cycles, 9, 359–372, 1995.

Ng, H. C., Cassarino, L., Pickering, R. A., Woodward, E. M. S., and Hendry, K. R.: Sediment efflux of silicon on the Greenland margin and implications for the marine silicon cycle. Earth Planet. Sci. Lett., 529, 115877, 2020.

Nielsen, S. G., Rehkämper, M., Teagle, D. A. H., Butterfield, D. A., Alt, J. C., and Halliday, A. N.: Hydrothermal fluid fluxes calculated from the isotopic mass balance of thallium in the ocean crust, Earth Planet. Sci. Lett., 251, 120–133, 2006.

Oelkers, E. H., Gislason, S. R., Eirıksdottir, E. S., Jones, M. T., Pearce, C. R., and Jeandel C.: The role of riverine particulate material on the global cycles of the elements, Appl. Geochem., 26, S365–S369, 2011.

Ohnemus, D. C., Rauschenberg, S., Krause, J. W., and Brezinski, M. A.: Silicon content of individual cells of *Synechococcus* from the North Atlantic Ocean, Mar. Chem., 187, 16–24, 2016.

Opalinka, B. and Cowlings, S. A.: Modelling the movement of biogenic silica from terrestrial vegetation to riverine systems within the continental USA, Ecol. Model., 312, 104–113, https://doi.org/10.1016/j.ecolmodel.2015.05.012, 2015.

Pasquier, B. and Holzer, M.: Inverse-model estimates of the ocean's coupled phosphorus, silicon, and iron cycles, Biogeosciences, 14, 4125–4159, https://doi.org/10.5194/bg-14-4125-2017, 2017.

Pearce, C. R., Jones, M. T., b, Oelkers, E. H., Pradoux, C., and Jeandel, C.: The effect of particulate dissolution on the neodymium (Nd) isotope and Rare Earth Element (REE) composition of seawater, Earth Planet. Sci. Lett., 369–370, 138–147, 2013.

Peng, T.-S. , Maier-Reimer, E., and Broecker, W. S.: Distribution of ^{32}Si in the world ocean: model compared to observation. Global Biogeochem. Cycles, 7, 464–474, 1993.

Philipps, A.: Modelling riverine dissolved silica on different spatial and temporal scales using statistical and machine learning methods, Ph.D thesis, Univ. Toronto, Canada, 121 pp., available at: http://hdl.handle.net/1807/101210, 2020.

Pickering, R. A., Cassarino, L., Hendry, K. R., Wang, X. L., Maiti, K., and Krause, J. W.: Using Stable Isotopes to Disentangle Marine Sedimentary Signals in Reactive Silicon Pools, Geophys. Res. Lett., 47, 1–11, https://doi.org/10.1029/2020GL087877, 2020.

Pondaven, P., Ragueneau, O., Tréguer, P., Hauvespre, A., Dezileau, L., and Reyss, J. L.: Resolving the 'opal paradox'in the Southern Ocean, Nature, 405, 168–172, 2000.

Prakash Babu, C., Brumsack, J., and Böttcher, M. E.: Barium as a productivity proxy in continental margin sediments: a study from the eastern Arabian Sea, Mar. Geol., 184, 189–206, 2002.

Rahman, S., Aller, R. C., Cochran, and J. K.: Cosmogenic ^{32}Si as a tracer of biogenic silica burial and diagenesis: Major deltaic sinks in the silica cycle, Geophys. Res. Lett., 43, 7124–7132, 2016.

Rahman, S., Aller, R. C., and Cochran, J. K.: The missing silica sink: revisiting the marine sedimentary Si cycle using cosmogenic ^{32}Si, Global Biogeochem. Cycles, 31, 1559–1578, 2017.

Rahman, S., Tamborski, J. J., Charette, M. A., and Cochran, J. K.: Dissolved silica in the subterranean estuary and the impact of submarine groundwater discharge on the global marine silica budget, Mar. Chem., 208, 29–42, 2019.

Roshan, S., DeVries, T., Wu, J., and Chen, G.: The internal cycling of Zinc in the ocean, Global Biogeochem. Cycles, 32, 1833–1849, 2018.

Saconne, L., Conley, D. J., Koning, E., Sauer, D., Sommer, M., Kaczorek, D., Blecher, S. W., and Kelly, E. F.: Assessing the extraction and quantification of amorphous silica in soils of forests and grassland ecosystems, Eur. J. Soil Sci., 58, 1446–1459, 2007.

Sarmiento, J. L. and Gruber, N.: Ocean biogeochemical dynamics, Princeton University Press, Princeton and Oxford, 2006.

Sarmiento, J. L., Simeon, J., Gnanadesikan, A., Gruber, N., Key, R. M., and Schlitzer, R.: Deep ocean biogeochemistry of silicic acid and nitrate, Global Biogeochem. Cycles, 21, GB1S90, 2007.

Siever, R.: Silica in the oceans: biological – geochemical interplay, in "Scientists in Gaia", edited by: Schneider, S. H. Boston, P. J., MIT Press, 285–295, 1991.

Struyf, E., Mörth, C.-M., Humborg, C., and Conley, D. J.: An enormous amorphous silica stock in boreal wetlands, J. Geophys. Res., 115, G04008, https://doi.org/10.1029/2010JG001324, 2010.

Syvistkia, J. P. M., Peckhama, S. D., Hilbermana, R., and Mulderb, T.: Predicting the terrestrial flux of sediment to the global ocean:a planetary perspective, Sediment. Geol., 162, 5–24, 2003.

Techer, I., Advocat, T., Lancelot, J., and Liotard, J. M.: Dissolution kinetics of basaltic glasses: Control by solution chemistry and protective effect of the alteration film, Chem. Geol., 176, 235–263, 2001.

Tegen, I. and Kohfeld, K. E.: Atmospheric Transport of Silicon, in: The silica cycle, human perturbations and impacts on aquatic 50 systems, edited by: Ittekot, V., Unger, D., Humborg, C., and Tac

An, N. T., 7, 81–91, The Silicon Cycle: Human Perturbations and Impacts on Aquatic Systems, Comm. Probl. Environ. (SCOPE) Ser. Vol. 66, Island Press, Washington, DC, 296 pp, 2006.

Tréguer, P. J.: The Southern Ocean silica cycle, C. R. Geosci., 346, 279–286, 2014.

Tréguer, P. J. and De La Rocha, C. L.: The World Ocean silica sycle, Annu. Rev. Mar. Sci., 5, 477–501, 2013.

Tréguer, P. J. and Jacques, G.: Dynamics of nutrients and phytoplankton, and fluxes of carbon, nitrogen and silica in the Antarctic ocean, Polar Biol., 12, 149–162, 1992.

Tréguer, P. J. and Pondaven P.: Silica control of carbon dioxide, Nature, 406, 358–359, 2000.

Tréguer, P. J., Louis Lindner, L., van Bennekom, A. J., Leynaert, A., Panouse, M., and Jacques, G.: Production of biogenic silica in the Weddell-Scotia Seas measured with ^{32}Si, Limnol. Oceanogr., 36, 1217–1227, 1991.

Tréguer, P. J., Nelson, D. M., Van Bennekom, A. J., Demaster, D. J., Leynaert,A., and Quéguiner, B.: The balance of silica in the world ocean, Science, 268, 376–79, 1995.

Tréguer, P. J., Bowler, C., Moriceau, B., Dutkiewicz, S., Gehlen, M., Aumont, O., Bittner, L., Dugdale, R., Finkel, Z., Iudicone, D., Jahn, O., Guidi, L., Lasbleiz, M., Leblanc, K., Levy, M., and Pondaven, P.: Influence of diatom diversity on the ocean biological carbon pump, Nat. Geosci., 11, 27–37, 2018.

Usbeck, U.: Modeling of marine biogeochemical cycles with an emphasis on vertical particle fluxes, PhD thesis, University Bremen, Germany, 1999.

Von Damm, K. L., Bischoff, J. L., and Rosenbauer, R. J.: Quartz solubility in hydrothermal seawater: An experimental study and equation describing quartz solubility for up to 0.5 M NaCl solutions, Am. J. Sci., 291, 977–1007, 1991.

Wang W., Yang, S., Ran, X., Liu, X.-M., Bataille, C. P., and Su, N.: Response of the Changjiang (Yangtze River) water chemistry to the impoundment of Three Gorges Dam during 2010–2011, Chem. Geol. 487, 1–11, 2018a.

Wang, X., Baskaran, M., Su, K., and Du, J.: The important role of submarine groundwater discharge (SGD) to derive nutrient fluxes into river dominated ocean margins – The East China Sea, Mar. Chem., 204, 121–132, 2018b.

Ward, B. A., Dutkiewicz, S., Jahn, O., and Follows, M. J.: A size-structured food-web model for the global ocean, Limnol. Oceanogr., 57, 1877–1891, 2012.

Westberry, T., Behrenfeld, M. J., Siegel, D. A., and Boss, E.: Carbon-based primary productivity modeling with vertically resolved photoacclimation, Global Biogeochem. Cycles, 22, GB2024, 2008.

Wheat, C. G. and McManus, J.: The potential role of ridge-flank hydrothermal systems on oceanic germanium and silicon balances, Geochim. Cosmochim. Acta, 69, 2021–2029, 2005.

Wheat, C. G. and Mottl, M. J.: Composition of pore and spring waters from Baby Bare: global implications of geochemical fluxes from a ridge flank hydrothermal system, Geochim. Cosmochim. Acta., 64, 629–642, 2000.

Wischmeyer, A. G., De La Rocha, C. L., Maier-Reimer, E., and Wolf-Gladrow, D. A.: Control mechanisms for the oceanic distribution of Si isotopes, Global Biogeochem. Cycles, 17, 1083, 2003.

Wollast, R., and Mackenzie, F. T.: Global biogeochemical cycles and climate, in: Climate Geosciences: A challenge for science and society in the 21st century, eds: Berger, A., Schneider, S., and Duplessy, J. C., Springer, Dordrecht, 453–473, 1989.

Yang S. L., Xu, K. H., Milliman, J. D., Yang, H. F., and Wu, C. S.: Decline of Yangtze River water and sediment discharge: Impact from natural and anthropogenic changes, Sci. Rep., 5, 12581, 2015.

Zhang, Z., Sun, X., Dai, M., Cao, Z., Fontorbe, G., and Conley, D. J.: Impact of human disturbance on the biogeochemical silicon cycle in a coastal sea revealed by silicon isotopes, Limnol. Oceanogr., 65, 515-528, 2019.

Zhao, B., Yao, P., Bianchi, T., and Xu, Y.: Early diagenesis and authigenic mineral formation in mobile muds of the Changjiang Estuary and adjacent shelf, J. Mar. Syst., 172, 64–74, 2017.